Homogeneous flux scheme for plasma simulation

Liu, L.

Award date:
2009

TECHNISCHE UNIVERSITEIT EINDHOVEN

Homogeneous Flux Scheme for Plasma Simulation

by

Lei Liu

Supervisors: Dr. Ir.J.H.M. ten Thije Boonkkamp and

Dr. Jan van Dijk

in the

CASA group

Department of Mathematics and Computer Science

July 2009

Abstract

This thesis has two parts. In the first part, we briefly introduce plasma physics. From fluid theory we give a mathematical model to simulate the dc discharge. Our model consists of conservation equations for ions and electrons and Poisson's equation for a self-consistent electric field. We discretize the equations in space by the finite volume-complete flux (FV-CF) scheme for the conservation equations and the central difference scheme for Poisson's equation. For time integration we use the implicit Euler method. The nonlinear system derived from discretization is solved by Newton's method and numerical results are presented. We get the results we expect and especially they are very similar with those given in literature. It shows that FV-CF scheme is a good method for the simulation of plasmas.

In the second part we present the homogeneous flux scheme for systems of advection-diffusion-reaction equations. Analysis and numerical experiments show that it is second-order accurate, expect for dominant advection. In this case the convergence order reduces to 1; however it can still approximate the exact solution very well.

Acknowledgements

I would like to express my gratitude to some people who were involved in this project.

First of all, my thanks go to my supervisor of seminar and final thesis Dr. Ir. J.H.M. ten Thije Boonkkamp. He arranged a comfortable schedule to work on this project and his deep knowledge on PDE theory and scientific computing gave me a lot of valuable guidance.

I also want to thank my other supervisor Dr. Jan van Dijk and PhD student Diana Mihailova from Department of Applied Physics. This project benefited greatly from their helps. They gave many advises from the view of Physics and helped me a lot to improve the results.

My thanks also go to my colleges in CASA group for the pleasant working environment.

I would like also to thank my friends Yabin Fan, Qingzhi Hou, Jie Liu and Sudhir for their support and help in study and daily life.

Finally, I want to thank my parents Junliang Liu and FengQin Yang and my girlfriend Jiahui Zhu for their consistent support.

Contents

List of Figures

List of Tables

Physical Constants

Mass of electron	m_{e}	=	9.109×10^{-31} kg
Mass of ion Helium	m_{i}	=	3.32×10^{-27} kg
Boltzmann's constant	K_{B}	=	1.381×10^{-23} m^2 kg s^{-2} K^{-1}
Permittivity of free space	ε_0	=	8.854×10^{-12} A^2 s^4 kg^{-1} m^{-3}
Permeability of free space	μ_0	=	$4\pi \times 10^{-7}$ N A^{-2}
Charge of an electron	e	=	-1.6×10^{-19} C

Chapter 1

Introduction to Plasma Physics

A plasma is an ionized gas consisting of positively and negatively charged particles with approximately equal charge densities. Plasmas can be produced by heating an ordinary gas to such a high temperature that the random kinetic energy of the molecules exceeds the ionization energy. Collisions then strip some of the electrons from the atoms, forming a mixture of electrons and ions. The plasma state is also referred to as the fourth state of matter. 99% of the matter in the universe is in the plasma state. Thus plasmas play a major role in the universe. Plasma physics is relevant to the formation of planetary radiation belts, the development of sunspots and solar flares and the generation of radio emissions from the Sun and other astrophysical objects, and so on. Numerous applications of basic plasma physics can be found in man-made devices. For example, fluorescent lights, electric arc welders and plasma etching machines are in common daily use. What makes plasmas particularly difficult to analyse is the fact that there is a big number of types of plasmas. The densities of the ions and electrons in plasmas can be in a large range. Plasmas behave sometimes like fluids, and sometimes like a collection of individual particles. For different plasmas we need different methods. Therefore we introduce two mathematical methods: fluid theory and kinetic theory. For more details see also [1, 2].

1.1 Plasmas as Fluids

In the fluid approximation we consider the plasma to be composed of two or more *interpenetrating fluids*, one for each species. In the simplest case, when there is only one species of ion, we shall need two equations of motion, one for the positively charged ion fluid and one for the negatively charged electron fluid. The neutral fluid will interact with the ions and electrons only through collisions. The ion and electron fluids will

interact with each other even in the absence of collisions, because of the electric and magnetic fields they generate.

The equation of motion for a single particle is

$$m\frac{d\boldsymbol{v}}{dt} = q(\boldsymbol{E} + \boldsymbol{v} \times \boldsymbol{B}), \tag{1.1}$$

where m is the mass, $\boldsymbol{v}$ the velocity and q the charge of the particle. $\boldsymbol{E}$ and $\boldsymbol{B}$ denote the electric field and magnetic field respectively. Assume first that there are no collisions and no thermal motions. Then all the particles in a fluid element move together, and the average velocity $\boldsymbol{u}$ of the particles in the element is the same as the individual particle velocity $\boldsymbol{v}$. The fluid equation is obtained simply by multiplying Eq. (1.1) by the density n

$$mn\frac{d\boldsymbol{u}}{dt} = qn(\boldsymbol{E} + \boldsymbol{u} \times \boldsymbol{B}). \tag{1.2}$$

In Eq. (1.1) the time derivative is to be taken at the position of the particles. We wish to have an equation for fluid elements fixed in space. So we change the derivative to convective derivative. Eq. (1.2) can be rewritten as

$$mn\left(\frac{\partial \boldsymbol{u}}{\partial t} + (\boldsymbol{u} \cdot \nabla)\boldsymbol{u}\right) = qn(\boldsymbol{E} + \boldsymbol{u} \times \boldsymbol{B}). \tag{1.3}$$

When thermal motions are taken into account, a pressure force has to be added to the right hand side of Eq. (1.3). This force arises from the random motion of particles in and out of a fluid element and does not appear in the equation for a single particle. Defining the pressure

$$p = nK_{\mathrm{B}}T, \tag{1.4}$$

where K_{B} is Boltzmann's constant and T the temperature, we have the fluid equation

$$mn\left(\frac{\partial \boldsymbol{u}}{\partial t} + (\boldsymbol{u} \cdot \nabla)\boldsymbol{u}\right) = qn(\boldsymbol{E} + \boldsymbol{u} \times \boldsymbol{B}) - \nabla p. \tag{1.5}$$

If there is a neutral gas, the charged fluid will exchange momentum with it through collisions. The momentum lost per collision will be proportional to the relative velocity $\boldsymbol{u} - \boldsymbol{u}_0$, where $\boldsymbol{u}_0$ is the velocity of the neutral fluid. If τ, the mean free time between collisions, is approximately constant, the resulting force term can be roughly written as $-mn(\boldsymbol{u} - \boldsymbol{u}_0)/\tau$. The equation of motion can be written as

$$mn\left(\frac{\partial \boldsymbol{u}}{\partial t} + (\boldsymbol{u} \cdot \nabla)\boldsymbol{u}\right) = qn(\boldsymbol{E} + \boldsymbol{u} \times \boldsymbol{B}) - \nabla p - \frac{mn(\boldsymbol{u} - \boldsymbol{u}_0)}{\tau}. \tag{1.6}$$

Collisions between charged particles have not been included. We will do it later.

Conservation of matter requires that the total number of particles N in a volume V can change only if there is a net flux of particles across the surface $\boldsymbol{S}$ bounding that volume. Since the particle flux density is $n\boldsymbol{u}$, we have, by the divergence theorem,

$$\frac{\mathrm{d}N}{\mathrm{d}t} = \int_V \frac{\partial n}{\partial t}\mathrm{d}V = -\oint_{\boldsymbol{S}} n\boldsymbol{u}\cdot\mathrm{d}\boldsymbol{S} = -\int_V \nabla\cdot(n\boldsymbol{u})\mathrm{d}V + \int_V s\mathrm{d}V, \tag{1.7}$$

where s is a source or sink of particles. Since this must hold for any volume V, the integrands must be equal:

$$\frac{\partial n}{\partial t} + \nabla\cdot(n\boldsymbol{u}) = s. \tag{1.8}$$

There is one such equation of continuity for each species.

One more relation is needed to close the system of equations. For this, we can use the thermodynamic equation of state relating p to n:

$$p = Cn^{\gamma}, \tag{1.9}$$

where C is a constant and γ is the ratio of specific heats.

For simplicity, let the plasma have only two species: ions and electrons. The charge and current densities ζ and $\boldsymbol{j}$ are then given by

$$\zeta = n_i q_i + n_e q_e, \tag{1.10a}$$

$$\boldsymbol{j} = n_i q_i \boldsymbol{v}_i + n_e q_e \boldsymbol{v}_e. \tag{1.10b}$$

where n_i, n_e are the densities of ions and electrons, respectively. Together with Maxwell's equations, Eq. (1.5), Eq. (1.8) and Eq. (1.9) we obtain the following set:

$$\varepsilon_0\nabla\cdot\boldsymbol{E} = \zeta, \tag{1.11}$$

$$\nabla\times\boldsymbol{E} = -\dot{\boldsymbol{B}}, \tag{1.12}$$

$$\nabla\cdot\boldsymbol{B} = 0, \tag{1.13}$$

$$\nabla\times\boldsymbol{B} = \mu_0(\boldsymbol{j} + \varepsilon_0\dot{\boldsymbol{E}}), \tag{1.14}$$

$$m_{\mathrm{s}}n_{\mathrm{s}}\left(\frac{\partial \boldsymbol{u}_{\mathrm{s}}}{\partial t} + (\boldsymbol{u}_{\mathrm{s}}\cdot\nabla)\boldsymbol{u}_{\mathrm{s}}\right) = q_{\mathrm{s}}n_{\mathrm{s}}(\boldsymbol{E} + \boldsymbol{u}_s\times\boldsymbol{B}) - \nabla p_{\mathrm{s}}, \quad \mathrm{s} = \mathrm{i},\ \mathrm{e}, \tag{1.15}$$

$$\frac{\partial n_{\mathrm{s}}}{\partial t} + \nabla\cdot(n_s\boldsymbol{u}_{\mathrm{s}}) = s, \quad \mathrm{s} = \mathrm{i},\ \mathrm{e}, \tag{1.16}$$

$$p_s = C_{\mathrm{s}}n_{\mathrm{s}}^{\gamma_{\mathrm{s}}}, \quad \mathrm{s} = \mathrm{i},\ \mathrm{e} \tag{1.17}$$

where ε_0 is the permittivity of free space and μ_0 the permeability of free space. There are 16 scalar unknowns: n_{i}, n_{e}, p_{i}, p_{e}, $\boldsymbol{v}_{\mathrm{i}}$, $\boldsymbol{v}_{\mathrm{e}}$, $\boldsymbol{E}$ and $\boldsymbol{B}$. There are apparently 18 scalar

equations if we count each vector equation as three scalar equations. However, two of Maxwell's equations are superfluous, since Eq. (1.11) and Eq. (1.13) can be recovered from the divergences of Eq. (1.12) and Eq. (1.14). The simultaneous solution of this set of 16 equations in unknowns gives a self-consistent set of fields and motions in the fluid approximation.

Any realistic plasma will have a density gradient, and the plasma will tend to diffuse toward regions of low density. We assume that the plasma is weakly ionized, so that charged particles collide primarily with neutral atoms rather than with one another. When an electron collides with a neutral atom, it may lose any fraction of its initial momentum, depending on the angle at which it rebounds. In a head-on collision with a heavy atom, the electron can lose twice its initial momentum, since its velocity reverses sign after the collision. The probability of momentum loss can be expressed in terms of the equivalent cross section σ that the atoms would have if they were perfect absorbers of momentum.

In Figure 1.1, electrons are incident upon a slab of area A and thickness $\mathrm{d}x$ containing n_n neutral atoms per m^3. The atoms are imagined to be opaque spheres of cross-sectional area σ; that is every time an electron comes within the area blocked by the atom, the electron loses all of its momentum. The number of atoms in the slab is $n_\mathrm{n} A \mathrm{d}x$.

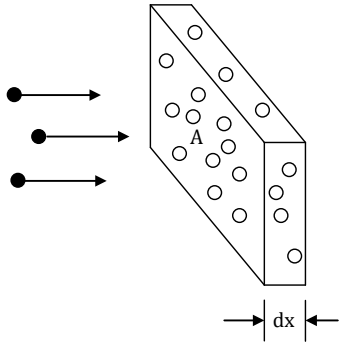

FIGURE 1.1: Illustration of the definition of cross section.

The fraction of the slab blocked by atoms is

$$n_\mathrm{n} A \sigma \mathrm{d}x / A = n_\mathrm{n} \sigma \mathrm{d}x,$$

where σ is the atom cross section. If a flux Γ of electrons is incident on the slab, the flux emerging on the other side is

$$\Gamma^* = \Gamma(1 - n_\mathrm{n} \sigma \mathrm{d}x).$$

Thus the change of Γ with distance $\mathrm{d}x$ is

$$\frac{\mathrm{d}\Gamma}{\mathrm{d}x} = -n_\mathrm{n}\sigma\Gamma$$

or

$$\Gamma = \Gamma_0 e^{-n_\mathrm{n}\sigma x} = \Gamma_0 e^{-x/\lambda_\mathrm{m}} \tag{1.18}$$

where Γ_0 is the incident flux. The quantity λ_m is the *mean free path* for collisions:

$$\lambda_\mathrm{m} = \frac{1}{n_\mathrm{n}\sigma}, \tag{1.19}$$

After traveling a distance λ_m, a particle will have had a good probability of making a collision. From (1.18) we have $\Gamma(\lambda_\mathrm{m})/\Gamma_0 = 1/e$. The mean free time, mean time between collisions for particles of velocity v, is given by

$$\tau = \frac{\lambda_\mathrm{m}}{v}, \tag{1.20}$$

and the mean frequency of collisions is

$$\tau^{-1} = \frac{v}{\lambda_\mathrm{m}} = n_\mathrm{n}\sigma v. \tag{1.21}$$

If we now average over particles of all velocities v in a Maxwellian distribution, we have what is generally called the collision frequency ν, i.e.,

$$\nu = n_\mathrm{n}\sigma\overline{v}. \tag{1.22}$$

The fluid equation of motion including collisions is

$$mn\left(\frac{\partial \boldsymbol{u}}{\partial t} + (\boldsymbol{u}\cdot\nabla)\boldsymbol{u}\right) = \pm qn\boldsymbol{E} - \nabla p - mn\nu\boldsymbol{u}, \tag{1.23}$$

where $\pm$ indicates the sign of the charge and we don't consider a magnetic field. We consider a steady state and neglect the inertia. Setting the left-hand side of (1.22) to 0, we have, for an isothermal plasma,

$$\begin{aligned}\boldsymbol{u} &= \frac{1}{mn\nu}\left(\pm qn\boldsymbol{E} - K_\mathrm{B}T\nabla n\right)\\ &= \pm\frac{q}{m\nu}\boldsymbol{E} - \frac{K_\mathrm{B}T}{m\nu}\frac{\nabla n}{n}.\end{aligned} \tag{1.24}$$

The coefficients above are called the *mobility* μ and the *diffusion coefficient* D, respectively:

$$\mu := \pm\frac{q}{m\nu}, \tag{1.25}$$

$$D := \frac{K_\mathrm{B}T}{m\nu}. \tag{1.26}$$

Note that $\mu < 0$ for electrons and $\mu > 0$ for ions. They are connected by the *Einstein relation*:

$$\mu = \pm\frac{qD}{K_\mathrm{B}T}. \tag{1.27}$$

With the help of these definitions, the flux Γ_j of the jth species can be written as

$$\Gamma_j := n_j \boldsymbol{u}_j = \mu_j n_j \boldsymbol{E} - D_j \nabla n. \tag{1.28}$$

1.2 Kinetic Theory

The fluid theory is the simplest description of a plasma; this approximation is sufficiently accurate to describe the majority of observed phenomena. There are some phenomena, for example, when the pressure is not high, for which a fluid treatment is inadequate. For these, we need to consider the velocity distribution function $f(\boldsymbol{v})$ for each species; this treatment is called kinetic theory. The density is a function of four scalar variables: $n = n(\boldsymbol{r}, t)$. When we consider velocity distributions, we have seven independent variables: $f = f(\boldsymbol{r}, \boldsymbol{v}, t)$. By $f(\boldsymbol{r}, \boldsymbol{v}, t)$, we mean that the number of particles per m^3 at position $\boldsymbol{r}$ and time t with velocity components between v_x and $v_x + \mathrm{d}v_x$, v_y and $v_y + \mathrm{d}v_y$, and v_z and $v_z + \mathrm{d}v_z$ is

$$f(x, y, z, v_x, v_y, v_z, t)\mathrm{d}v_x\mathrm{d}v_y\mathrm{d}v_z.$$

The integral of this is:

$$n(\boldsymbol{r}, t) = \int_{-\infty}^{+\infty} f(\boldsymbol{r}, \boldsymbol{v}, t)\mathrm{d}\boldsymbol{v}. \tag{1.29}$$

The corresponding normalized probability density function $\hat{f}$ satisfies

$$\int_{-\infty}^{+\infty} \hat{f}(\boldsymbol{r}, \boldsymbol{v}, t)\mathrm{d}\boldsymbol{v} = 1, \tag{1.30}$$

clearly,

$$f(\boldsymbol{r}, \boldsymbol{v}, t) = n(\boldsymbol{r}, t)\hat{f}(\boldsymbol{r}, \boldsymbol{v}, t). \tag{1.31}$$

A particularly important distribution function is the Maxwellian:

$$\hat{f}_\mathrm{m} = (m/2\pi K_\mathrm{B}T)^{3/2} \exp(-v^2/v_\mathrm{th}^2), \tag{1.32}$$

where

$$v := (v_x^2 + v_y^2 + v_z^2)^{1/2} \quad \text{and} \quad v_{\text{th}} := (2K_{\text{B}}T/m)^{1/2}.$$

There are several average velocities of a Maxwellian distribution that are commonly used. The root-mean-square velocity is given by

$$(\overline{v^2})^{1/2} = (3K_{\text{B}}T/m)^{1/2}. \tag{1.33}$$

The average magnitude of the velocity $\bar{v}$ is found as

$$\bar{v} = \int_{-\infty}^{+\infty} v\hat{f}_{\text{m}}(\boldsymbol{v})\mathrm{d}v = (8K_{\text{B}}T/\pi m)^{1/2}. \tag{1.34}$$

The velocity component in a single direction, say v_x, has a different average. For an isotropic distribution $\bar{v}_x$ vanishes, but $\overline{|v_x|}$ not:

$$\overline{|v_x|} = (2K_{\text{B}}T/\pi m)^{1/2}.$$

The random flux crossing an imaginary plane perpendicular with x-axis from one side to the other is given by

$$\Gamma_{\text{random}} = \frac{1}{2}n\overline{|v_x|} = \frac{1}{4}n\bar{v}. \tag{1.35}$$

Here we have used Eq. (1.34) and the fact that only half of the particles cross the plane in either direction.

The fundamental equation which $f(\boldsymbol{r}, \boldsymbol{v}, t)$ has to satisfy is the Boltzmann equation:

$$\frac{\partial f}{\partial t} + \boldsymbol{v} \cdot \nabla f + \frac{\boldsymbol{F}}{m} \cdot \frac{\partial f}{\partial \boldsymbol{v}} = \left(\frac{\partial f}{\partial t}\right)_c, \tag{1.36}$$

where $\boldsymbol{F}$ is the force acting on the particles, and $(\partial f/\partial t)_c$ is the time rate of change of f due to collisions. The total derivative of f with time is

$$\frac{\mathrm{d}f}{\mathrm{d}t} = \frac{\partial f}{\partial t} + \frac{\partial f}{\partial x}\frac{\mathrm{d}x}{\mathrm{d}t} + \frac{\partial f}{\partial y}\frac{\mathrm{d}y}{\mathrm{d}t} + \frac{\partial f}{\partial z}\frac{\mathrm{d}z}{\mathrm{d}t} + \frac{\partial f}{\partial v_x}\frac{\mathrm{d}v_x}{\mathrm{d}t} + \frac{\partial f}{\partial v_y}\frac{\mathrm{d}v_y}{\mathrm{d}t} + \frac{\partial f}{\partial v_z}\frac{\mathrm{d}v_z}{\mathrm{d}t},$$

where $\frac{\partial f}{\partial t}$ is the explicit dependence on time. The next three terms are just $\boldsymbol{v} \cdot \nabla f$. With the help of Newton's law $m\frac{\mathrm{d}\boldsymbol{v}}{\mathrm{d}t} = \boldsymbol{F}$, the last three terms are recognized as $(\boldsymbol{F}/m) \cdot (\partial f/\partial \boldsymbol{v})$. The total derivative $\mathrm{d}f/\mathrm{d}t$ can be interpreted as the rate of change as seen in a frame moving with the particles. $\mathrm{d}f/\mathrm{d}t$ is the convective derivative in phase space. The Boltzmann equation simply says that $\mathrm{d}f/\mathrm{d}t$ is zero unless there are collisions.

In a sufficiently hot plasma, collisions can be neglected. If the force $\boldsymbol{F}$ is entirely electromagnetic, Eq. (1.36) takes the special form

$$\frac{\partial f}{\partial t} + \boldsymbol{v} \cdot \nabla f + \frac{q}{m}(\boldsymbol{E} + \boldsymbol{v} \times \boldsymbol{B}) \cdot \frac{\partial f}{\partial \boldsymbol{v}} = 0, \tag{1.37}$$

which is called the *Vlasov equation*. Because of its comparative simplicity, this is the equation most commonly studied in kinetic theory. When there are collisions with neutral atoms, the collision term in Eq. (1.36) can be approximated by

$$\left(\frac{\partial f}{\partial t}\right)_c = \frac{f_n - f}{\tau},$$

where f_n is the distribution function of the neutral atoms and τ is a constant collision time. This is called a *Krook collision term*. It is the kinetic generalization of the collision term in Eq. (1.22).

The fluid equations in Section 1.1 are simply moments of the Boltzmann equation. The lowest moment is obtained by integrating Eq. (1.36) from $-\infty$ to ∞ with $\boldsymbol{F}$ equal to the Lorentz force:

$$\int \frac{\partial f}{\partial t}\mathrm{d}\boldsymbol{v} + \int \boldsymbol{v} \cdot \nabla f \mathrm{d}\boldsymbol{v} + \frac{q}{m}\int (\boldsymbol{E} + \boldsymbol{v} \times \boldsymbol{B}) \cdot \frac{\partial f}{\partial \boldsymbol{v}}\mathrm{d}\boldsymbol{v} = \int \left(\frac{\partial f}{\partial t}\right)_c \mathrm{d}\boldsymbol{v}$$

The first term gives

$$\int \frac{\partial f}{\partial t}\mathrm{d}\boldsymbol{v} = \frac{\partial}{\partial t}\int f \mathrm{d}\boldsymbol{v} = \frac{\partial n}{\partial t}.$$

Since $\boldsymbol{v}$ is in dependent variable and therefore is not affected by the operator ∇, the second term gives

$$\int \boldsymbol{v} \cdot \nabla f \mathrm{d}\boldsymbol{v} = \nabla \cdot \int \boldsymbol{v} f \mathrm{d}\boldsymbol{v} = \nabla \cdot (n\bar{\boldsymbol{v}}) := \nabla \cdot (n\boldsymbol{u}),$$

where the average velocity $\boldsymbol{u}$ is the fluid velocity by definition. The $\boldsymbol{E}$-term vanishes for the following reason:

$$\int \boldsymbol{E} \cdot \frac{\partial f}{\partial \boldsymbol{v}}\mathrm{d}\boldsymbol{v} = \int \frac{\partial}{\partial \boldsymbol{v}} \cdot (f\boldsymbol{E})\mathrm{d}\boldsymbol{v} = \int_{S_\infty} f\boldsymbol{E} \cdot \mathrm{d}\boldsymbol{S}.$$

The perfect divergence is integrated to give the value of $f\boldsymbol{E}$ on the surface S_∞ at $v = \infty$. This vanishes if $f \to 0$ faster than v^{-2} as $v \to \infty$, as is necessary for any distribution with finite energy. The $\boldsymbol{v} \times \boldsymbol{B}$ term can be written as follows:

$$\int (\boldsymbol{v} \times \boldsymbol{B}) \cdot \frac{\partial f}{\partial \boldsymbol{v}}\mathrm{d}\boldsymbol{v} = \int \frac{\partial}{\partial \boldsymbol{v}} \cdot (f\boldsymbol{v} \times \boldsymbol{B})\mathrm{d}\boldsymbol{v} - f\frac{\partial}{\partial \boldsymbol{v}} \cdot (\boldsymbol{v} \times \boldsymbol{B})\mathrm{d}\boldsymbol{v} = 0.$$

The first integral can again be converted to a surface integral. For a Maxwellian, f falls

faster than any power of v as $v \to \infty$, and the integral therefore vanishes. The second integral vanishes because $\boldsymbol{v} \times \boldsymbol{B}$ is perpendicular to $\partial/\partial \boldsymbol{v}$. Finally, the fourth term vanishes because collisions cannot change the total number of particles(recombination is not considered here). Then we obtain the *equation of continuity*:

$$\frac{\partial n}{\partial t} + \nabla \cdot (n\boldsymbol{u}) = 0. \tag{1.38}$$

The next moment of the Boltzmann equation is obtained by multiplying Eq. (1.36) by $m\boldsymbol{v}$ and integrating over $\mathrm{d}\boldsymbol{v}$. We obtain the *fluid equation of motion*

$$mn\left(\frac{\partial \boldsymbol{u}}{\partial t} + (\boldsymbol{u} \cdot \nabla)\boldsymbol{u}\right) = qn(\boldsymbol{E} + \boldsymbol{u} \times \boldsymbol{B}) - \nabla \cdot \boldsymbol{P} + \boldsymbol{P}_{ij}. \tag{1.39}$$

where $\boldsymbol{P}_{ij}$ is the momentum gain of the ith particle fluid caused by collisions with jth particle. This equation describes the flow of momentum. To treat the flow of energy, we may take the next moment of the Boltzmann equation by multiplying by $\frac{1}{2}m\boldsymbol{v} \cdot \boldsymbol{v}$ and integrating. We then obtain the heat flow equation.

Chapter 2

Mathematical Model

We aim at simulating a discharge space like in Figure 2.1 to understand the cathode fall and negative glow regions of dc discharges. After the plasma gets to steady state the discharge space is separated into three regions: positive column, negative glow and cathode fall. The discharge is sustained by the secondary emission of electrons from the cathode due primarily to positive ion bombardment. The secondary electrons leave the cathode and are accelerated in the cathode fall because of the high electric field to high energies and ionize neutrals there. The new created electrons are also accelerated. Because at high energies electrons tend to forward scatter, the energetic electrons continue to propagate into the low-field region of the discharge, resulting in ionization in negative glow. Since there are no energetic particles hitting the anode, there is no secondary emission from the anode. The goal of our mathematical model is to represent these processes. We present a fluid model which is based on a fluid representation of the charged particles. The model consists of two transport equations for ions and electrons and Poisson's equation for a self-consistent electric field.

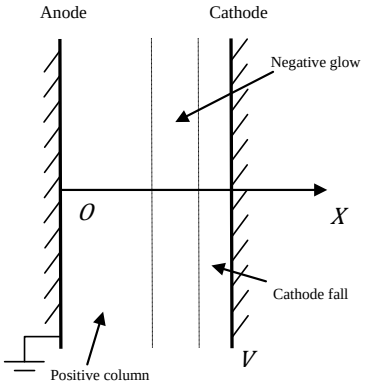

FIGURE 2.1: Discharge space geometry

2.1 Assumptions of the Model

The gas is assumed to be weakly ionized. The two electrodes are infinitely large and the distance between them is l. There is an external direct-current potential applied to the electrodes. We assume the anode is connected to ground and the potential is V on the cathode. We also assume that the background gas Helium is cold, i.e., we neglect the interactions between the charged particles and neutral atoms. Only electron impact ionization from the ground state will be considered

$$e + \mathrm{He} \rightarrow \mathrm{He}^+ + 2e,$$

so there are three species in the chamber: electrons, ions He^+ and atoms He. Atoms He are abundant. Electron-ion recombination is also neglected. Under the assumption of low ionization degree the temperature T_{gas}, pressure p and density N of the background gas are assumed to be constant and unaffected by the discharge. Moreover the density of particles $n_{\mathrm{e}}, n_{\mathrm{i}} \ll N$. Indices e and i refer to electrons and positive ions, respectively. The density $n_{\mathrm{e,(i)}}(x,t)$ is the number of electrons (ions) per m^3 at position x and time t. Particle transport is described by the continuity equations and the drift-diffusion momentum transport equations. Particle inertia is thus neglected. The electron diffusion coefficient D_{e} and mobility μ_{e} are supposed to satisfy the Einstein relation

$$D_{\mathrm{e}}/\mu_{\mathrm{e}} = K_{\mathrm{B}} T_{\mathrm{e}}/e = \frac{2}{3}\varepsilon_{\mathrm{e}}/e,$$

where $\varepsilon_{\mathrm{e}} = \frac{3}{2} K_{\mathrm{B}} T_{\mathrm{e}}$ is the electron mean energy, K_{B} Boltzmann's constant, T_{e} the electron temperature and e the charge of an electron. Because the ion mass is almost equal to that of the neutral gas atoms the ions are cooled efficiently by the background gas, thus the temperature of ions $T_{\mathrm{i}} \approx T_{\mathrm{gas}} = \mathrm{const}$.

2.2 Equations

The following notation is used. $m_{\mathrm{e,(i)}}$ is the electron (ion) mass, $\boldsymbol{E}(x,t)$ is the electric field, furthermore $V(x,t)$ the electric potential in the discharge and K is the electron impact ionization rate. D_{i} and μ_{i} denote the ion diffusion coefficient and mobility, respectively. $\boldsymbol{\Gamma}_{\mathrm{e,(i)}}$ is the electron (ion) flux. Using the notation and the assumptions above, the charged particles transport equations can be written as follows

Positive ions:

$$\frac{\partial n_\mathrm{i}}{\partial t} + \nabla \cdot \mathbf{\Gamma}_\mathrm{i} = n_\mathrm{e} N K, \tag{2.1a}$$

$$\mathbf{\Gamma}_\mathrm{i} = \mu_\mathrm{i} \boldsymbol{E} n_\mathrm{i} - D_\mathrm{i} \nabla n_\mathrm{i}, \quad \mu_\mathrm{i} > 0. \tag{2.1b}$$

electrons:

$$\frac{\partial n_\mathrm{e}}{\partial t} + \nabla \cdot \mathbf{\Gamma}_\mathrm{e} = n_\mathrm{e} N K, \tag{2.2a}$$

$$\mathbf{\Gamma}_\mathrm{e} = \mu_\mathrm{e} \boldsymbol{E} n_\mathrm{e} - D_\mathrm{e} \nabla n_\mathrm{e}, \quad \mu_\mathrm{e} < 0. \tag{2.2b}$$

electric field:

$$\boldsymbol{E} = -\nabla V, \tag{2.3a}$$

$$\nabla \cdot (\varepsilon_0 \boldsymbol{E}) = -\nabla \cdot (\varepsilon_0 \nabla V) = q(n_\mathrm{i} - n_\mathrm{e}), \tag{2.3b}$$

where ε_0 is the vacuum permittivity and $q > 0$ the elementary charge.

We can write the equations Eqs. (2.1)-(2.3) in 1-D as

Positive ions:

$$\frac{\partial n_\mathrm{i}}{\partial t} + \frac{\partial \Gamma_\mathrm{i}}{\partial x} = n_\mathrm{e} N K, \tag{2.4a}$$

$$\Gamma_\mathrm{i} = \mu_\mathrm{i} E n_\mathrm{i} - D_\mathrm{i} \frac{\partial n_\mathrm{i}}{\partial x}, \quad \mu_\mathrm{i} > 0. \tag{2.4b}$$

Electrons:

$$\frac{\partial n_\mathrm{e}}{\partial t} + \frac{\partial \Gamma_\mathrm{e}}{\partial x} = n_\mathrm{e} N K, \tag{2.5a}$$

$$\Gamma_\mathrm{e} = \mu_\mathrm{e} E n_\mathrm{e} - D_\mathrm{e} \frac{\partial n_\mathrm{e}}{\partial x}, \quad \mu_\mathrm{e} < 0. \tag{2.5b}$$

electric field:

$$E = -\frac{\mathrm{d}V}{\mathrm{d}x}, \tag{2.6a}$$

$$\frac{\mathrm{d}}{\mathrm{d}x}(\varepsilon_0 E) = -\varepsilon_0 \left(\frac{\mathrm{d}^2 V}{\mathrm{d}x^2} \right) = q(n_\mathrm{i} - n_\mathrm{e}), \tag{2.6b}$$

In the expression of fluxes Γ the first term gives the flux due to the electric field (drift) and the second term represents the flux due to concentration gradients (diffusion). The set of equations above is similar to the systems used in a number of papers on discharge modeling [3–6]. The values used are presented in Table 2.1. Electron and ion transport

coefficients are assumed to be independent of the energy distribution function. The ionization coefficient is a function of the reduced electric field E/N.

NAME	NOTATION	VALUE	UNITS
Density of electrons	n_e		m^{-3}
Density of ions	n_i		m^{-3}
Electric field	$\boldsymbol{E}$		V/m
Electric potential	V		V
Temperature of gas	T_gas	300	K
Temperature of electrons	T_e	2×11600	K
Pressure of gas	p	1	Torr
Distance between two electrodes	l	0.4	m
Density of gas	N	3×10^{22}	m^{-3}
Mobility of electrons	μ_e	-70	$\mathrm{m}^2\mathrm{V}^{-1}\mathrm{s}^{-1}$
Mobility of ions	μ_i	0.85	$\mathrm{m}^2\mathrm{V}^{-1}\mathrm{s}^{-1}$
Diffusion coefficient of electrons	D_e	350	$\mathrm{m}^2\mathrm{s}^{-1}$
Diffusion coefficient of ions	D_i	0.03	$\mathrm{m}^2\mathrm{s}^{-1}$
Electron impact ionization rate	K		$\mathrm{m}^3\mathrm{s}^{-1}$
Voltage applied on the cathode	V	-400	Volt
secondary emission coefficient	γ_i	0.2	

TABLE 2.1: Variables and constants in the model

2.3 Boundary Conditions

We use the boundary condition like in [5, 7, 8]. Ions have two components in the boundary flux, i.e., a drift flux due to the electric field and a diffusion flux. Besides a drift and a diffusion flux Electrons has a flux due to secondary emission. The flux directed towards the electrodes is given by

$$\boldsymbol{\Gamma}_\mathrm{s} \cdot \boldsymbol{n} = a\mu_\mathrm{s}(\boldsymbol{E} \cdot \boldsymbol{n})n_\mathrm{s} + \frac{1}{4}v_{\mathrm{th,\ s}}n_\mathrm{s}, \quad \mathrm{s} = \mathrm{e,\ i}, \tag{2.7}$$

where $\boldsymbol{n}$ is unit outward normal and $v_\mathrm{th,s}$ is the thermal velocity of species, given by

$$v_{\mathrm{th,\ s}} = \left(\frac{8K_\mathrm{B}T_\mathrm{s}}{\pi m_\mathrm{s}}\right)^{1/2}. \tag{2.8}$$

The number a is set to 1 if the drift velocity $\mu_{\mathrm{s}}\boldsymbol{E}$ is directed towards the electrodes and to 0 otherwise, i.e.,

$$a = \begin{cases} 1 & \text{if } \mu_{\mathrm{s}}\boldsymbol{E}\cdot\boldsymbol{n} > 0, \\ \\ 0 & \text{if } \mu_{\mathrm{s}}\boldsymbol{E}\cdot\boldsymbol{n} \leq 0. \end{cases} \tag{2.9}$$

For electrons, a flux due to secondary emission is added to the flux defined in Eq.(2.9), i.e.,

$$\boldsymbol{\Gamma}_{\mathrm{e}}\cdot\boldsymbol{n} = a\mu_{\mathrm{e}}(\boldsymbol{E}\cdot\boldsymbol{n})n_{\mathrm{e}} + \frac{1}{4}v_{\mathrm{th,\,e}}n_{\mathrm{e}} - \gamma_{\mathrm{i}}\boldsymbol{\Gamma}_{\mathrm{i}}\cdot\boldsymbol{n}, \tag{2.10}$$

where the secondary emission coefficient γ_{i} is the average number of electrons emitted per incident ion. For the Poisson equation Eq. (2.8) we use Dirichlet boundary conditions.

The boundary conditions (2.7) and (2.10) can be written in 1-D as following:

The flux of ions on the left boundary $x = 0$

$$\Gamma_i = (\mu_{\mathrm{i}}\min(E,0) - \frac{1}{4}v_{\mathrm{th,\,i}})n_{\mathrm{i}}, \tag{2.11}$$

and on the right boundary $x = l$

$$\Gamma_i = (\mu_{\mathrm{i}}\max(E,0) + \frac{1}{4}v_{\mathrm{th,\,i}})n_{\mathrm{i}}. \tag{2.12}$$

The flux of ions on the left boundary $x = 0$

$$\Gamma_e = (\mu_{\mathrm{e}}\max(E,0) - \frac{1}{4}v_{\mathrm{th,\,e}})n_{\mathrm{e}} - \gamma_i\Gamma_i, \tag{2.13}$$

and on the right boundary $x = l$

$$\Gamma_e = (\mu_{\mathrm{e}}\min(E,0) + \frac{1}{4}v_{\mathrm{th,\,e}})n_{\mathrm{e}} - \gamma_i\Gamma_i. \tag{2.14}$$

Chapter 3

Spatial Discretization and Time Integration

In this chapter we discretise the equations in the mathematical model. We discretise the continuity equations Eq. (2.4a) and Eq. (2.5a) in space by the finite volume-complete flux (FV-CF) scheme [9] and Poisson equation Eq. (2.6) by the second-order central difference scheme.

3.1 Grid Points on the Boundary

We cover the interval between the two electrodes with a finite number of disjunct intervals (control volumes) I_j of size Δx as shown in Figure 3.1. We choose the grid point x_j where the variables $n_{\mathrm{e\ (,\ i)}}$ have to be approximated in the center of the jth interval I_j. Consequently we have $I_j = [x_{j-1/2}, x_{j+1/2}]$ with $x_{j+1/2} = \frac{1}{2}(x_j + x_{j+1})$.

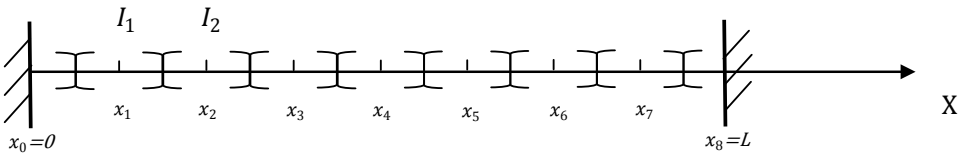

FIGURE 3.1: Interface points on the boundary

The continuity equations Eqs. (2.4a) and (2.5a) can be uniformly written as

$$\frac{\partial n_{\mathrm{s}}}{\partial t} + \frac{\partial \Gamma_{\mathrm{s}}}{\partial x} = n_{\mathrm{e}} N K, \tag{3.1a}$$

$$\Gamma_{\mathrm{s}} = \mu_{\mathrm{s}} E n_{\mathrm{s}} - D_{\mathrm{s}} \frac{\partial n_{\mathrm{s}}}{\partial x}, \tag{3.1b}$$

where s = i or e. We use the notation in [9]. The Peclet number $P := \frac{\mu_s E}{D_s}\Delta x$ and $\varepsilon = D_s$. The numerical flux $F_{j+1/2}$ which is based on the boundary value problem on $[x_j, x_{j+1}]$ has the form

$$F_{j+1/2} = \alpha_{j+1/2} n_j - \beta_{j+1/2} n_{j+1} + \eta_{j+1/2} s_j + \delta_{j+1/2} s_{j+1}, \tag{3.2}$$

where s_j is the source term $n_e NK$ restricted on the grid point x_j and the coefficients $\alpha_{j+1/2}$ etc. only depend on $\mu_s E$ and D_s and are given by

$$\begin{aligned}
\alpha_{j+1/2} &:= \tfrac{\mathcal{E}_{j+1/2}}{\Delta x} B^-_{j+1/2}, \quad \beta_{j+1/2} := \tfrac{\mathcal{E}_{j+1/2}}{\Delta x} B^+_{j+1/2}, \\
\eta_{j+1/2} &:= \max\left(\tfrac{1}{2} - W^+_{j+1/2}, 0\right)\Delta x, \quad \delta_{j+1/2} := \min\left(\tfrac{1}{2} - W^+_{j+1/2}, 0\right)\Delta x, \\
\mathcal{E}_{j+1/2} &:= \tfrac{\widetilde{P}_{j+1/2}}{\bar{P}_{j+1/2}} \widetilde{\varepsilon}_{j+1/2}, \; B^\pm_{j+1/2} := B(\pm \bar{P}_{j+1/2}), \; W^+_{j+1/2} := W(\bar{P}_{j+1/2}),
\end{aligned} \tag{3.3}$$

where the average $\bar{a}_{j+1/2}$ and the weighted average $\widetilde{a}_{j+1/2}$ on $[x_j, x_{j+1}]$ are defined as follows

$$\bar{a}_{j+1/2} := \frac{1}{2}(a_j + a_{j+1}), \tag{3.4a}$$

$$\widetilde{a}_{j+1/2} := W(-\bar{P}_{j+1/2}) a_j + W(\bar{P}_{j+1/2}) a_{j+1}. \tag{3.4b}$$

The Bernoulli function B and the function W are defined by

$$B(z) = \frac{z}{e^z - 1}, \quad W(z) := \frac{e^z - 1 - z}{z(e^z - 1)}. \tag{3.5}$$

The transport term is discretized as:

$$\left(\frac{\partial \Gamma}{\partial x}\right)_j = \frac{F_{j+1/2} - F_{j-1/2}}{\Delta x}. \tag{3.6}$$

We adopt the following notation: variables defined in the grid points x_i and x_{i+1} are indicated with the subscripts C(center) and E(east), respectively. After the substitution of the finite volume-complete flux scheme (3.2), the discretized continuity equation for the grid points in the interior has the following form

$$\frac{\mathrm{d}n_j}{\mathrm{d}t}\Delta x - a_{W,j} n_{j-1} + a_{C,j} n_j - a_{E,j} n_{j+1} = b_{W,j} s_{j-1} + b_{C,j} s_j + b_{E,j} s_{j+1}, \tag{3.7}$$

where the coefficients $a_{W,j}, b_{W,j}$ etc. are defined by

$$\begin{aligned}
a_{W,j} &:= \alpha_{j-1/2}, \quad a_{E,j} := \beta_{j+1/2}, \quad a_{C,j} := \alpha_{j+1/2} + \beta_{j-1/2}, \\
b_{W,j} &:= \eta_{j-1/2}, \quad b_{E,j} := -\delta_{j+1/2}, \quad b_{C,j} := \Delta x - \eta_{j+1/2} + \delta_{j-1/2}.
\end{aligned} \tag{3.8}$$

For the grid points on the boundary we have to use the boundary condition Eq. (2.9)

and Eq. (2.12) and apply the FV-CF scheme on an half interval. For electrons the boundary flux is

$$\Gamma_e = (\mu_{\mathrm{e}} \max(E, 0) - \frac{1}{4} v_{\mathrm{th,\,e}}) n_{\mathrm{e}} - \gamma_i \Gamma_i, \tag{3.9}$$

on the left boundary $x = 0$. Substitution of this expression in the FV-CF scheme we obtain the semi-discretized continuity equation:

$$\frac{\mathrm{d}n_{\mathrm{e},0}}{\mathrm{d}t} \frac{\Delta x}{2} + a_{C,0} n_{\mathrm{e},0} - a_{E,0} n_{\mathrm{e},1} = b_{C,0} s_0 + b_{E,0} s_1 - \gamma_{\mathrm{i}} \Gamma_{\mathrm{i},0}, \tag{3.10}$$

with the coefficients

$$\begin{aligned} a_{E,0} := \beta_{1/2}, \quad a_{C,0} := \alpha_{1/2} - \mu_{\mathrm{e}} \max(E_0, 0) + \frac{1}{4} v_{\mathrm{th,\,e}}, \\ b_{E,0} := -\delta_{1/2}, \quad b_{C,0} := \Delta x/2 - \eta_{1/2}. \end{aligned} \tag{3.11}$$

The expression for the right boundary $x = l$ is analogous. For the ions the secondary-emission terms are omitted from Eq. (3.8) and Eq. (3.9) and note the difference in the first term between the ions flux and electrons flux.

3.2 Interface Points not on the Boundary

We can also choose the grid points like in Figure 3.2. Except for the first and last interval the discretization is the same as in Section 3.1.

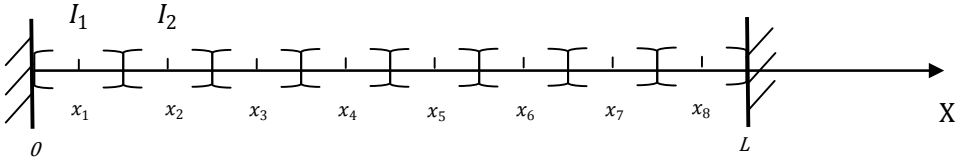

FIGURE 3.2: Grid Points not on the Boundary

For the first grid point we apply FV-CF scheme on the first cell I_1. For electron the boundary flux is given in Eq. (3.8). Substitution of this expression in the FV-CF scheme we obtain the semi-discretized continuity equation:

$$\begin{aligned} &\frac{\mathrm{d}n_{\mathrm{e},1}}{\mathrm{d}t} \Delta x + \alpha_{3/2} n_{\mathrm{e},1} - \beta_{3/2} n_{\mathrm{e},2} + \eta_{3/2} s_1 + \delta_{3/2} s_2 \\ &- a \mu_{\mathrm{e}} E n_{\mathrm{e},1/2} + \frac{1}{4} v_{\mathrm{th,\,e}} n_{\mathrm{e},1/2} + \gamma_{\mathrm{i}} \Gamma_{\mathrm{i},1/2} = s_1 \Delta x. \end{aligned} \tag{3.12}$$

We need the values of n_e and n_i on the boundary but the boundary points are not grid points. By linear extrapolation we can write $n_{\mathrm{e},1/2} = \frac{3}{2} n_{\mathrm{e},1} - \frac{1}{2} n_{\mathrm{e},2}$ and $n_{\mathrm{i},1/2} =$

$\frac{3}{2}n_{\mathrm{i},1} - \frac{1}{2}n_{\mathrm{i},2}$. Thus the semi-discretized continuity equation can be written as

$$\frac{\mathrm{d}n_{\mathrm{e},1}}{\mathrm{d}t}\Delta x + a_{C,1}n_{\mathrm{e},1} - a_{E,1}n_{\mathrm{e},2} = b_{C,1}s_1 + b_{E,1}s_2 - \gamma_{\mathrm{i}}F_{\mathrm{i},1/2}, \tag{3.13}$$

with the coefficients

$$\begin{aligned} a_{E,1} := \beta_{3/2} - a\tfrac{1}{2}\mu_{e,1}E_1 + \tfrac{1}{8}v_{\mathrm{th,\,e}}, \quad a_{C,1} := \alpha_{3/2} - a\tfrac{3}{2}\mu_{e,1}E_1 + \tfrac{3}{8}v_{\mathrm{th,\,e}}, \\ b_{E,1} := -\delta_{3/2}, \quad b_{C,1} := \Delta x - \eta_{3/2}. \end{aligned} \tag{3.14}$$

and $F_{\mathrm{i},1/2} = (a\mu_{\mathrm{e}}E - \frac{1}{4}v_{\mathrm{th,\,e}})(\frac{3}{2}n_{\mathrm{i},1} - \frac{1}{2}n_{\mathrm{i},2})$. The expression for the right boundary point is analogous. For ions the secondary-emission terms are omitted form Eq. (3.11) and Eq. (3.12) and note the difference in the first term between the ions flux and electrons flux. In our calculations, we use the first discretization method in Section 3.1. There are two reasons: First, we have the exact expression of flux on the boundary in the first method, while we have to extrapolate the value of density on the boundary in the second method. Second, it is more convenient for Poisson's equation because of the Dirichlet boundary condition. Although we discretise the transport equations by FV-CF scheme, for simplicity we use the homogeneous flux scheme in the calculation. Homogeneous flux scheme is a special case of FV-CF scheme. The terms related with the source term in the expression of the numerical flux (3.2) are omitted.

3.3 Central Scheme for Poisson equation

We choose the grid points like in Figure 3.1. At grid point x_j applying the second-order central difference scheme to Eq. (2.6) we have

$$-\frac{V_{j+1} - 2V_j + V_{j-1}}{\Delta x^2} = \frac{q}{\varepsilon_0}(n_{\mathrm{i},j} - n_{\mathrm{e},j}). \tag{3.15}$$

Because of the Dirichlet boundary on the left boundary we have

$$2V_1 - V_2 = V_0 + \Delta x^2 \frac{q}{\varepsilon_0}(n_{\mathrm{i},1} - n_{\mathrm{e},1}). \tag{3.16}$$

On the right boundary we have

$$-V_{N_x-2} + 2V_{N_x-1} = V_{N_x} + \Delta x^2 \frac{q}{\varepsilon_0}(n_{\mathrm{i},N_x-1} - n_{\mathrm{e},N_x-1}). \tag{3.17}$$

where V_0 and V_n are the values on the boundary and N_x is the number of grid points.

3.4 Time Integration

We use the implicit Euler method [10] as the time integrator because it may circumvent the time-restrictions encountered in an explicit treatment. Consider the initial-value problem

$$y' = f(x, y), \quad y(a) = \alpha. \tag{3.18}$$

The implicit Euler method can be expressed as

$$y_{j+1} = y_j + hf(x_{j+1}, y_{j+1}), \tag{3.19}$$

where h is time step and y_i is the approximation of $y(x_i)$. After applying the implicit Euler method the continuity equations can be written as ($n = n_\mathrm{e}$ or $n = n_\mathrm{i}$)

$$(n^{k+1} - n^k)/\Delta t = \mathcal{L}(n^{k+1}, V^{k+1}) + S^{k+1}, \tag{3.20}$$

where S^{k+1} is the source term at the new time level and $\mathcal{L}$ represents the spatial operator for transport term.

In the discretized Poisson's equation the densities at the previous time level ($l = k$) or the new time level ($l = k + 1$) can be used,

$$\left(\frac{\varepsilon_0}{q}\right) \frac{V_{j+1}^{k+1} - 2V_j^{k+1} + V_{j-1}^{k+1}}{\Delta x^2} = n_\mathrm{e}^{l_\mathrm{e}} - n_\mathrm{i}^{l_\mathrm{i}}, \tag{3.21}$$

where l_e, $l_\mathrm{i} = k$ or $k + 1$ which includes different couplings between the transport equations and Poisson's equation. We choose $l_\mathrm{e} = k + 1$ and $l_\mathrm{i} = k$ and end up with a nonlinear system for n_e^{k+1} and V^{k+1}:

$$n_\mathrm{e}^{k+1} - \Delta t\mathcal{L}(n_\mathrm{e}^{k+1}, V^{k+1}) - \Delta t n_\mathrm{e}^{k+1} NK = n_\mathrm{e}^k, \tag{3.22a}$$

$$\left(\frac{\varepsilon_0}{q}\right) \frac{V_{j+1}^{k+1} - 2V_j^{k+1} + V_{j-1}^{k+1}}{\Delta x^2} = n_\mathrm{e}^{k+1} - n_\mathrm{i}^k, \tag{3.22b}$$

and a linear equation for the ion density:

$$n_\mathrm{i}^{k+1} - \Delta t\mathcal{L}(n_\mathrm{i}^{k+1}, V^{k+1}) = n_\mathrm{i}^k + \Delta t n_\mathrm{e}^{k+1} NK, \tag{3.23}$$

where V^{k+1} and n_e^{k+1} are known from Eq. (3.22). For each time step we first solve the nonlinear system (3.22) by Newton's method. Then we use the values obtained of n_e and V to solve the linear system (3.23) to obtain the values of n_i.

Chapter 4

Numerical Solution Methods

In this chapter we discuss some methods to efficiently solve nonlinear systems. We first introduce Newton's method which is the simplest and most widely used iterative method and then we investigate the embedding of the considered nonlinear system into a time dependent ODE-system.

4.1 Newton's Method

Consider the nonlinear system

$$\boldsymbol{F}(\boldsymbol{x}) = 0, \tag{4.1}$$

where $\boldsymbol{F}(\boldsymbol{x}) = (f_1(\boldsymbol{x}), \cdots, f_n(\boldsymbol{x}))^{\mathrm{T}}$ with a root $\boldsymbol{x}^* = (x_1^*, \cdots, x_n^*)$. Newton's method arises from linearizing $\boldsymbol{F}(\boldsymbol{x})$. Expanding $\boldsymbol{F}(\boldsymbol{x})$ around an approximation $\boldsymbol{x}^i$ of $\boldsymbol{x}^*$ gives the linear expression

$$\boldsymbol{G}(\boldsymbol{x}) := \boldsymbol{F}(\boldsymbol{x}^i) + \boldsymbol{J}(\boldsymbol{x}^i)(\boldsymbol{x} - \boldsymbol{x}^i), \tag{4.2}$$

where

$$\boldsymbol{J}(\boldsymbol{x}) := \begin{bmatrix} \frac{\partial f_1}{\partial x_1} & \cdots & \frac{\partial f_1}{\partial x_n} \\ \vdots & & \vdots \\ \frac{\partial f_n}{\partial x_1} & \cdots & \frac{\partial f_n}{\partial x_n} \end{bmatrix} \tag{4.3}$$

is the Jacobi matrix of $\boldsymbol{F}(\boldsymbol{x})$. Let $\boldsymbol{G}(\boldsymbol{x}) = 0$ and if $\boldsymbol{J}(\boldsymbol{x}^i)$ is non-singular, we can obtain a series of approximations of $\boldsymbol{x}^*$ defined as

$$\boldsymbol{x}^{i+1} = \boldsymbol{x}^i - \boldsymbol{J}^{-1}(\boldsymbol{x}^i)\boldsymbol{F}(\boldsymbol{x}^i), \quad i = 0, 1, 2, \ldots \tag{4.4}$$

given an initial guess $\boldsymbol{x}^0$. Newton's method is known to give local second order convergence [11], i.e.

$$\|\boldsymbol{x}^* - \boldsymbol{x}^{i+1}\| = \mathcal{O}(\|\boldsymbol{x}^* - \boldsymbol{x}^i\|^2), \quad i \to \infty. \tag{4.5}$$

Although it has good convergence properties and simplicity Newton's method is not without drawbacks. First, the initial guess should be very close to the sought solution. In fact it's convergence region can be very small. Second, each iteration of the method is rather expensive, requiring an evaluation of the Jacobi matrix and the solution of a linear system. Continuation methods [11] can be used to find a good initial guess. The idea is to solve first a simpler "nearby" problem. The solution obtained is then used to produce an improved starting point for the original one. To improve the convergence behavior, damped Newton method is a good choice. The idea is to control the step size which is taken in the Newton direction to reduce the number of iteration. For reducing the cost of the Newton iteration we can fix the Jacobi matrix for a few iteration. In the next section we introduce a solution strategy that is based on embedding the original system into an initial value problem.

4.2 The Mixed Euler Method

4.2.1 Derivation

Consider the *Davidenko* equation

$$\frac{\mathrm{d}\boldsymbol{x}}{\mathrm{d}\tau} = -\boldsymbol{J}^{-1}(\boldsymbol{x})\boldsymbol{F}(\boldsymbol{x}), \tag{4.6a}$$

$$\boldsymbol{x}(0) = \boldsymbol{x}_0, \tag{4.6b}$$

with τ an artificial time. Applying the explicit Euler scheme to Eq. (4.6) with a step size $\lambda_i = \tau_{i+1} - \tau_i$ we obtain

$$\boldsymbol{x}^{i+1} = x^i - \lambda_i \boldsymbol{J}^{-1}(\boldsymbol{x}^i)\boldsymbol{F}(\boldsymbol{x}^i), \tag{4.7}$$

where $\boldsymbol{x}^i$ is numerical approximation of $\boldsymbol{x}(\tau_i)$. Eq. (4.7) is exactly the damped Newton method. This implies that improving robustness for the damped Newton method applied to the original nonlinear system (4.1) translates into improving stability of the explicit Euler scheme applied to the system (4.6). We should note that the final goal is not to obtain an accurate temporal evolution of $\boldsymbol{x}(\tau)$, but to reach a steady state solution of the ODE system (4.6). So we choose the time step as large as possible as long as it doesn't jeopardize the stability. the implicit Euler method satisfies our requirements.

Applying it to system (4.6) we obtain

$$\boldsymbol{x}^{i+1} = x^i - \lambda_i \boldsymbol{J}^{-1}(\boldsymbol{x}^{i+1})\boldsymbol{F}(\boldsymbol{x}^{i+1}). \tag{4.8}$$

It has a big computational cost, i.e. both $\boldsymbol{F}(\boldsymbol{x})$ and $\boldsymbol{J}^{-1}(\boldsymbol{x})$ have to be evaluated at the new time level. The situation can be improved if we replace $\boldsymbol{J}^{-1}(\boldsymbol{x}^{i+1})$ by $\boldsymbol{J}^{-1}(\boldsymbol{x}^i)$. Eq. (4.8) is written in a mix form called the *mixed Euler* formula

$$\boldsymbol{x}^{i+1} = x^i - \lambda_i \boldsymbol{J}^{-1}(\boldsymbol{x}^i)\boldsymbol{F}(\boldsymbol{x}^{i+1}). \tag{4.9}$$

The iteration method (4.9) is computationally less expensive than (4.8). It is still consistent of order one and its stability properties are similar to those of the implicit Euler method [12].

System (4.9) is again nonlinear and will be solved by applying Newton's method. It can be written as

$$\boldsymbol{G}(\boldsymbol{z}) = \boldsymbol{z} - x^i + \lambda_i \boldsymbol{J}^{-1}(\boldsymbol{x}^i)\boldsymbol{F}(\boldsymbol{z}) = 0. \tag{4.10}$$

After applying Newton's method we obtian

$$\boldsymbol{z}^{l+1} = \boldsymbol{z}^l - (\boldsymbol{I} + \lambda_i \boldsymbol{J}^{-1}(\boldsymbol{x}^i)\boldsymbol{J}(\boldsymbol{z}^l))^{-1}\boldsymbol{G}(\boldsymbol{z}^l). \tag{4.11}$$

In the iteration the evaluation of the Jacobi matrix is computed for every new approximation $\boldsymbol{z}^{l+1}$. Since this would be very expensive, we replace $\boldsymbol{J}(\boldsymbol{z}^l)$ by $\boldsymbol{J}(\boldsymbol{x}^i)$, i.e. we freeze the Jacobi matrix in the inner iteration. (4.11) reduces to

$$\boldsymbol{z}^{l+1} = \frac{\lambda_i}{1+\lambda_i}(\boldsymbol{z}^l - \boldsymbol{J}^{-1}(\boldsymbol{x}^i)\boldsymbol{F}(\boldsymbol{z}^l)) + \frac{1}{1+\lambda_i}\boldsymbol{x}^i. \tag{4.12}$$

Thus our method consists of two iteration levels: the outter one given by (4.9) whose iterations determine the temporal evolution of $\boldsymbol{x}$, and the inner one (4.12) to calculate (4.9).

4.2.2 Step Size Control

An important issue for the Mixed Euler method is the control of the step size λ_i. A reasonable way to do this is to choose the time steps such that the discretisation error does not exceed a certain fixed tolerance. In this subsection we introduce two techniques to decide the time step for each step: step size control via the second derivative approximation and step size control via extrapolation.

We would like to determine the step size such that the integral of the discretisation error over a time interval remains approximately bounded, i.e.

$$|\lambda_i \delta_i(\lambda_i)| \approx \text{TOL}, \tag{4.13}$$

where $\delta_i(\lambda_i)$ is the local truncation error at τ_i and TOL is the desired tolerance. We can't calculate the value of $|\lambda_i \delta_i(\lambda_i)|$ directly, but we can find some expressions to approximate it. The first candidate is the estimate of the local truncation error to evaluate numerically the second derivative of the function $\boldsymbol{x}(\tau)$. It can be shown that

$$\text{EST} := \lambda_i^2 \left| \frac{\|\boldsymbol{x}^i - \boldsymbol{x}^{i-1}\|}{\lambda_{i-1}} - \frac{\|\boldsymbol{x}^{i-1} - \boldsymbol{x}^{i-2}\|}{\lambda_{i-2}} \right| \cdot \frac{1}{\lambda_{i-1} + \lambda_{i-2}} \approx |\lambda_i \delta_i(\lambda_i)|. \tag{4.14}$$

Another candidate is to control step size via extrapolation. We try to approximate δ by comparing two solutions computed from different time steps: one that reaches τ_{i+1} in one step of length $\lambda_i = \tau_{i+1} - \tau_i$ the solution is denoted by $\boldsymbol{x}_{i+1}$, the other that reaches τ_{i+1} in two steps equal to $\lambda_i/2$ the solution is denoted by $\hat{\boldsymbol{x}}_{i+1}$; see Figure 4.1.

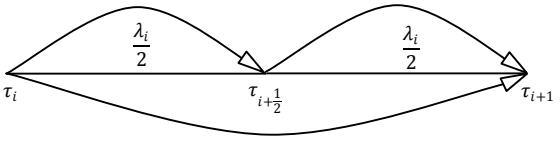

FIGURE 4.1: The solution calculated by different time steps

Using the Davidenko equation, the solution $\hat{\boldsymbol{x}}^{i+1}$ reads

$$\begin{aligned} \hat{\boldsymbol{x}}^{i+1} &= \hat{\boldsymbol{x}}^{i+1/2} - \frac{\lambda_i}{2} \boldsymbol{J}^{-1}(\hat{\boldsymbol{x}}^{i+1/2}) \boldsymbol{F}(\hat{\boldsymbol{x}}^{i+1}) \\ &= \boldsymbol{x}^i - \frac{\lambda_i}{2} \boldsymbol{J}^{-1}(\boldsymbol{x}^i) \boldsymbol{F}(\hat{\boldsymbol{x}}^{i+1/2}) - \frac{\lambda_i}{2} \boldsymbol{J}^{-1}(\hat{\boldsymbol{x}}^{i+1/2}) \boldsymbol{F}(\hat{\boldsymbol{x}}^{i+1}) \end{aligned} \tag{4.15}$$

It can be shown, see [13], that

$$\text{EST} := 2\|\hat{\boldsymbol{x}}^{i+1} - \boldsymbol{x}^{i+1}\| \approx |\lambda_i \delta_i(\lambda_i)|. \tag{4.16}$$

In the following algorithm, EST is required to satisfy

$$\text{EST} \leq \text{ATOL} + \text{RTOL} \cdot \|\boldsymbol{x}^{i+1}\|, \tag{4.17}$$

where ATOL and RTOL are an absolute and a relative tolerance, respectively. The values ATOL and RTOL determine the accuracy with which the temporal evolution of

the system is computed and are up to the user. Now we present a modification of the algorithm given [13], by using (4.14). The algorithm called Implicit Euler-Extrapolation Algorithm (IE/EA) by using (4.16) is similar.

Mixed Euler algorithm (MEA)

1. Let $\boldsymbol{x}^0$ be given;
2. For $i = 0, 1$
   * Set $\lambda_i = \frac{1}{1+\|\boldsymbol{F}(\boldsymbol{x}^i)\|}$;
   * Solve (4.9) for $\boldsymbol{x}^{i+1}$ using (4.12);
     - Let the number of Newton iterations $l = m_1$. It is not necessary to make the Newton iteration convergent;
3. For $i = 2, 3, \ldots$
   * Set $\lambda_i = \lambda_{i-1}$;
   * Solve (4.9) for $\boldsymbol{x}^{i+1}$ using (4.12), using $\|\boldsymbol{z}^{l+1} - \boldsymbol{z}^l\|_\infty \leq \text{TolInt}$ as the stopping criterion of the internal iteration;
     - If the Newton process (4.12) does not converge after $l = m_1$ iterations, set $\lambda_i = \frac{1}{2}\lambda_i$ and continue iterating until either convergence or $l = m_2$;
   * Compute EST with (4.14);
   * Evaluate the test funcition

$$\text{TEST} := \frac{\text{EST}}{\text{ATOL} + \text{RTOL} \cdot \|\boldsymbol{x}^{i+1}\|}; \tag{4.18}$$

   * If $\frac{1}{\rho} \leq \text{TEST} \leq \rho$ the solution $\boldsymbol{x}^{i+1}$ is accepted;
   * If $\text{TEST} > \rho$ the discretisation error is too big, the solution $\boldsymbol{x}^{i+1}$ is rejected and a new solution is computed after updating λ_i according to

$$\lambda_i := \alpha \frac{\lambda_i}{\sqrt{\text{TEST}}}; \tag{4.19}$$

   * If $\text{TEST} < \frac{1}{\rho}$ the temporal evolution is too accurate: the new solution $\boldsymbol{x}^{i+1}$ is accepted and the step size is increased according to (4.18);
   * If λ_i has not been changed for the last n iterations, set $\lambda_i = 2\lambda_i$.
   * If $\text{TEST} < \rho$ check the stop criterion $\|\boldsymbol{J}^{-1}(\boldsymbol{x}^i)\boldsymbol{F}(\boldsymbol{x}^{i+1})\|$ of the external iteration (4.9).

The values of ρ, n, m_1 and m_2 can be arbitrarily chosen. α is a safety coefficient used to deal with severe nonlinearities. It is usually set equal to 0.9.

4.3 Numerical Experiments

In this section we use some benchmark problems to assess the performance of the methods introduced in Section 4.2. We use $n = m_1 = 3$, $m_2 = 10$, $\rho = 4$ and $\alpha = 1$. The stopping criterion of the external iteration is $\|\boldsymbol{J}^{-1}(\boldsymbol{x}^i)\boldsymbol{F}(\boldsymbol{x}^{i+1})\| \leq 10^{-6}$. For the first two examples ATOL = RTOL = 10^{-1} and ATOL = RTOL = 10^{-2} for the third example. Moreover let TolInt = 10^{-1} for the stopping criterion of internal iteration.

Example 1

Consider the function, see [14]

$$\boldsymbol{F}(\boldsymbol{x}) := \begin{pmatrix} x_1^2 - x_2 + 1 \\ x_1 - \cos(\frac{\pi x_2}{2}) \end{pmatrix}, \tag{4.20}$$

with solution $\boldsymbol{x}^* = (0,1)^{\mathrm{T}}$. We use $\boldsymbol{x}^0 = (1,0)^{\mathrm{T}}$ and $\boldsymbol{x}^0 = (-1,-1)^{\mathrm{T}}$ as initial guess. Figures 4.2 and 4.3 show the path of the solutions computed with the two different algorithms for the two initial guess, respectively.

Example 2

The second problem, see [13], is

$$\boldsymbol{F}(\boldsymbol{x}) := \begin{pmatrix} \frac{1}{2}\sin(x_1 x_2) - \frac{x_2}{4\pi} - \frac{x_1}{2} \\ \left(1 - \frac{1}{4\pi}\right)(e^{2x_1} - e) + \frac{e x_2}{\pi} - 2e x_1 \end{pmatrix}. \tag{4.21}$$

Its solution is $\boldsymbol{x}^* = (0.5, \pi)^{\mathrm{T}}$. We use $\boldsymbol{x}^0 = (0.6, 3)^{\mathrm{T}}$ as initial guess, see Figure 4.4.

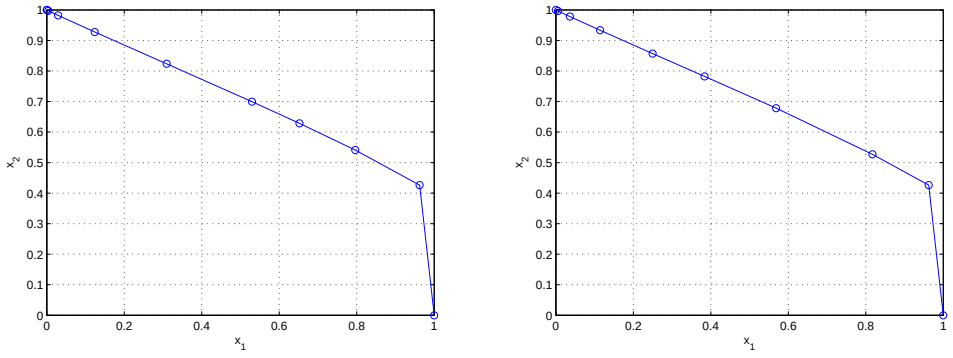

(a) MEA (b) BDF1/EA

FIGURE 4.2: Transient behavior from the initial guess $\boldsymbol{x}^0 = (1,0)^{\mathrm{T}}$ to the steady state solution $\boldsymbol{x}^* = (0,1)^{\mathrm{T}}$

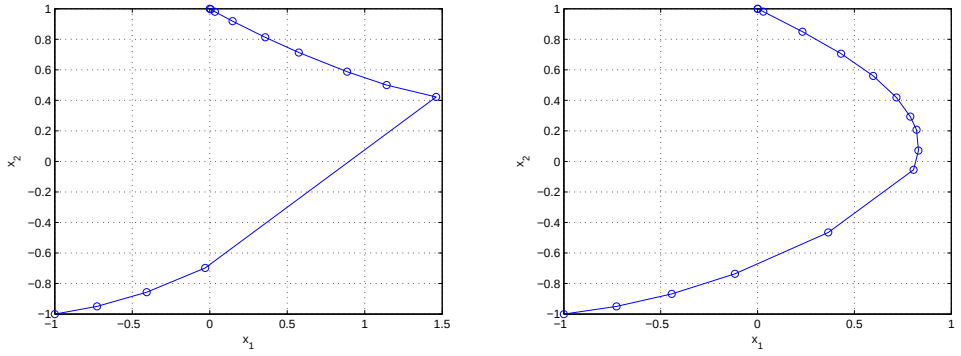

(a) MEA (b) BDF1/EA

FIGURE 4.3: Transient behavior from the initial guess $\boldsymbol{x}^0 = (-1, -1)^{\mathrm{T}}$ to the steady state solution $\boldsymbol{x}^* = (0, 1)^{\mathrm{T}}$

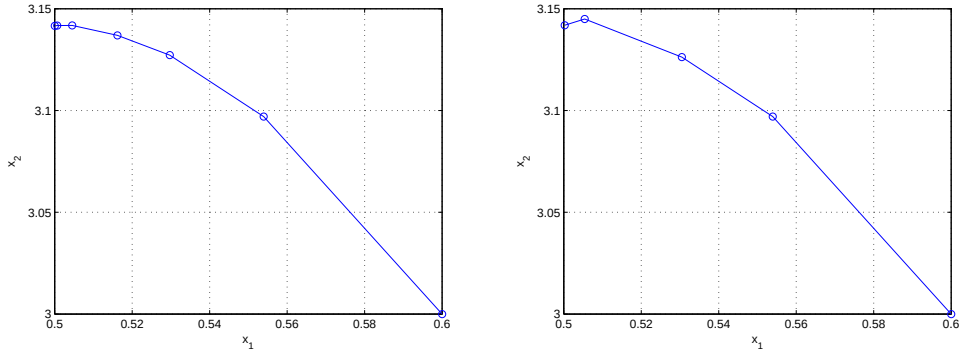

(a) MEA (b) BDF1/EA

FIGURE 4.4: Transient behavior from the initial guess $\boldsymbol{x}^0 = (0.6, 3)^{\mathrm{T}}$ to the steady state solution $\boldsymbol{x}^* = (0.5, \pi)^{\mathrm{T}}$

Example 3

The final problem, see [13], is

$$\boldsymbol{F}(\boldsymbol{x}) := \begin{pmatrix} 400x_1(x_1^2 - x_2) + 2(x_1 - 1) \\ -200(x_1^2 - x_2) \end{pmatrix}, \tag{4.22}$$

whose solution is $\boldsymbol{x}^* = (1, 1)^{\mathrm{T}}$. We use $\boldsymbol{x}^0 = (-1.2, 1)^{\mathrm{T}}$ and as $\boldsymbol{x}^0 = (6, 6)^{\mathrm{T}}$ initial guess. From Figure 4.5 and 4.6 we can see that the solution, from whichever point we start, moves towards the parabola $x_1^2 = x_2$ to which the exact solution belong and the parabola is very close to the curve $x_1^2 = x_2 - 0.005$, where the Jacobi matrix is singular; see also [12, 13].

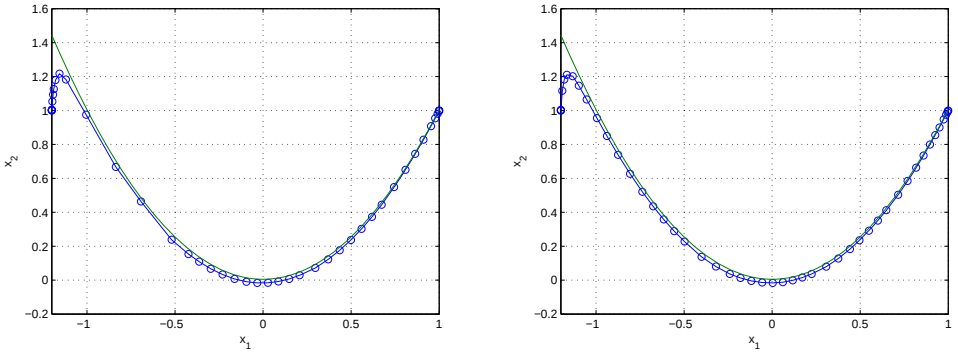

(a) MEA (b) BDF1/EA

FIGURE 4.5: Transient behavior from the initial guess $\boldsymbol{x}^0 = (-1.2, 1)^{\mathrm{T}}$ to the steady state solution $\boldsymbol{x}^* = (1, 1)^{\mathrm{T}}$

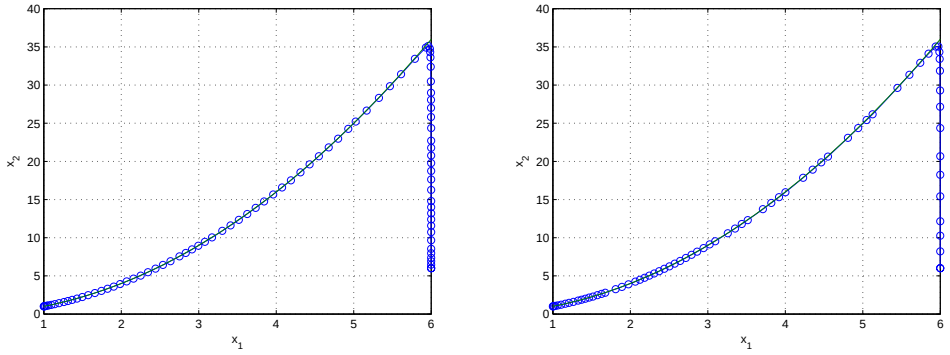

(a) MEA (b) BDF1/EA

FIGURE 4.6: Transient behavior from the initial guess $\boldsymbol{x}^0 = (6, 6)^{\mathrm{T}}$ to the steady state solution $\boldsymbol{x}^* = (1, 1)^{\mathrm{T}}$

Chapter 5

Numerical Results

After discretizing the continuity equations and Poisson equation in space and integrating by implicit Euler method we can solve the systems obtained in Chapter 3 by Newton's method presented in Chapter 4. In Section 5.1 we check the validity of the homogeneous flux scheme for our model and in section 5.2 we present some numerical results of the mathematical model.

5.1 Numerical Experiment of Steady Problem

To check the validity of the homogeneous flux scheme for our model we consider the following steady problem

$$\frac{\partial \Gamma_{\mathrm{i}}}{\partial x} = n_{\mathrm{e}} N K, \tag{5.1a}$$

$$\Gamma_{\mathrm{i}} = \mu_{\mathrm{i}} E n_{\mathrm{i}} - D_{\mathrm{i}} \frac{\partial n_{\mathrm{i}}}{\partial x}, \qquad \mu_{\mathrm{i}} > 0. \tag{5.1b}$$

$$\frac{\partial \Gamma_{\mathrm{e}}}{\partial x} = n_{\mathrm{e}} N K, \tag{5.2a}$$

$$\Gamma_{\mathrm{e}} = \mu_{\mathrm{e}} E n_{\mathrm{e}} - D_{\mathrm{e}} \frac{\partial n_{\mathrm{e}}}{\partial x}, \qquad \mu_{\mathrm{e}} < 0. \tag{5.2b}$$

$$E = -\frac{\partial V}{\partial x}, \tag{5.3a}$$

$$\frac{\partial}{\partial x}(\varepsilon_0 E) = -\frac{\partial}{\partial x}\left(\varepsilon_0 \frac{\partial V}{\partial x}\right) = q(n_{\mathrm{i}} - n_{\mathrm{e}}), \tag{5.3b}$$

The boundary conditions are Dirichlet conditions for three equations. If we let $q = 0$ in Eq. (5.3b) then we are able to solve it analytically. In Figure 5.1 the exact solutions of Eq. (5.3) are presented. V is linear and E is a constant. Using the value E obtained we can solve (5.1) and (5.2) analytically. In Figure 5.2 we compare the numerical solutions with the analytical solutions. In the calculations the coefficients are just chosen for easy calculations not from our model. We see that the numerical solutions coincide with the analytical solutions very well. That means our discretization method in space is suitable for our model.

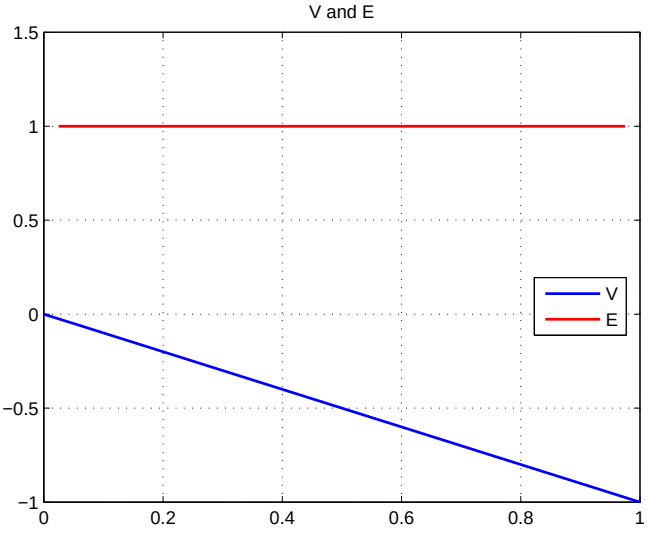

FIGURE 5.1: Exact solution for V and E when $q = 0$

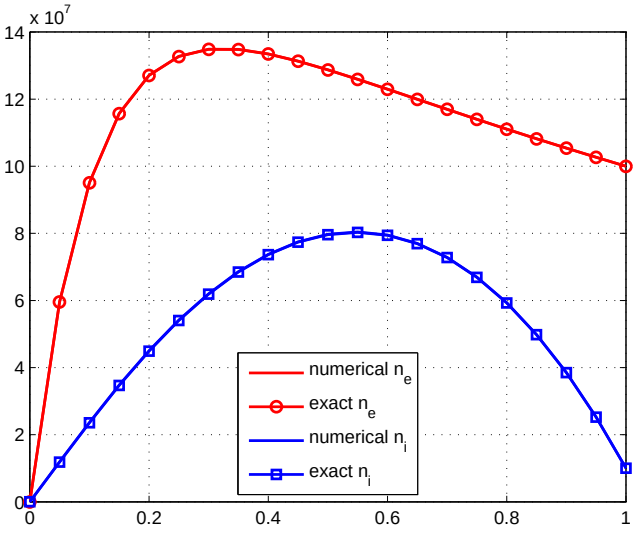

FIGURE 5.2: Comparison between numerical and exact solutions of n_e and n_i when $q = 0$

5.2 Numerical Results of the Mathematical Model

In this section we present the numerical results. The values of the parameters used here are given in Table 2.1. The initial of the densities $n_e = n_i = 10^{12}$ m^{-3}. The length of the grid interval and time step are 4×10^{-3} m and 10^{-10} s, respectively. The ionization coefficient is a function of the reduced electric field which is interpolated by the data given by Dr. Jan van Dijk in department of Applied Physics, see Figure 5.3.

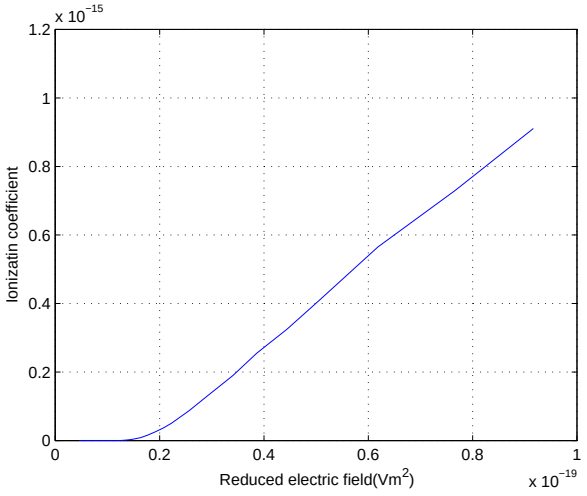

FIGURE 5.3: The ionization coefficient

The results after different time periods are shown in Figure 5.4-5.7. In those figures the one on the top is the distribution of potential; the one in the middle is the distribution of electric field and the one on the bottom is the distribution of densities of ions and electrons.

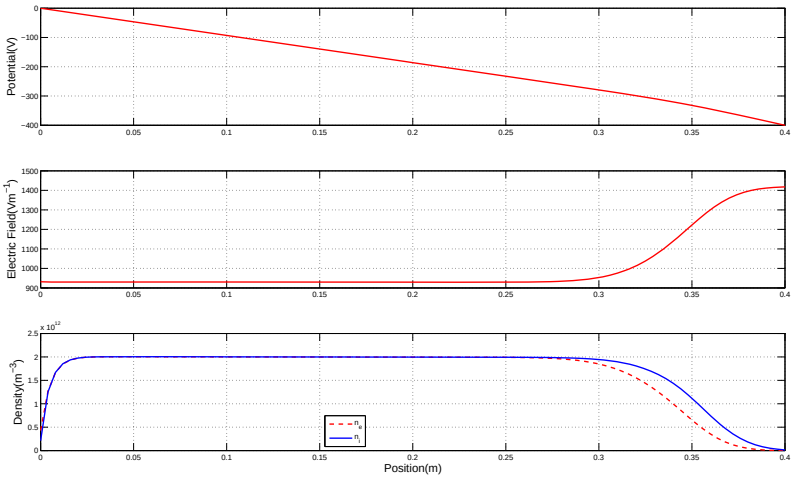

FIGURE 5.4: The results after 10^4 time steps

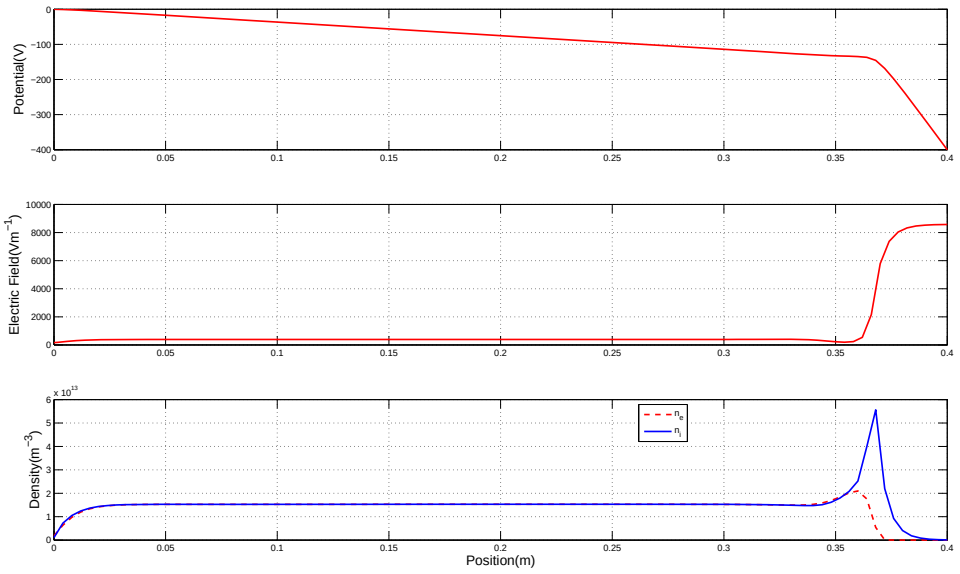

FIGURE 5.5: The results after 2×10^4 time steps

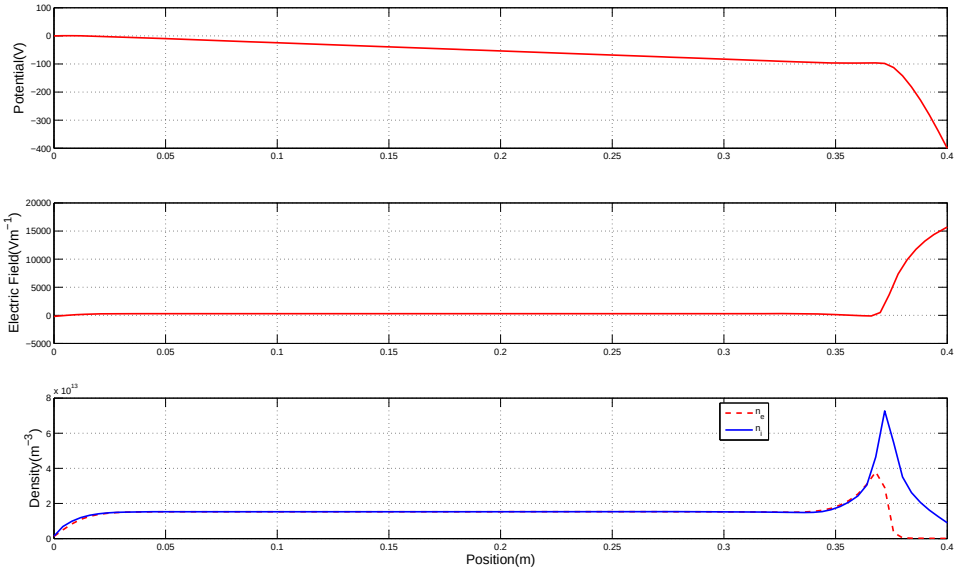

FIGURE 5.6: The results after 4×10^4 time steps

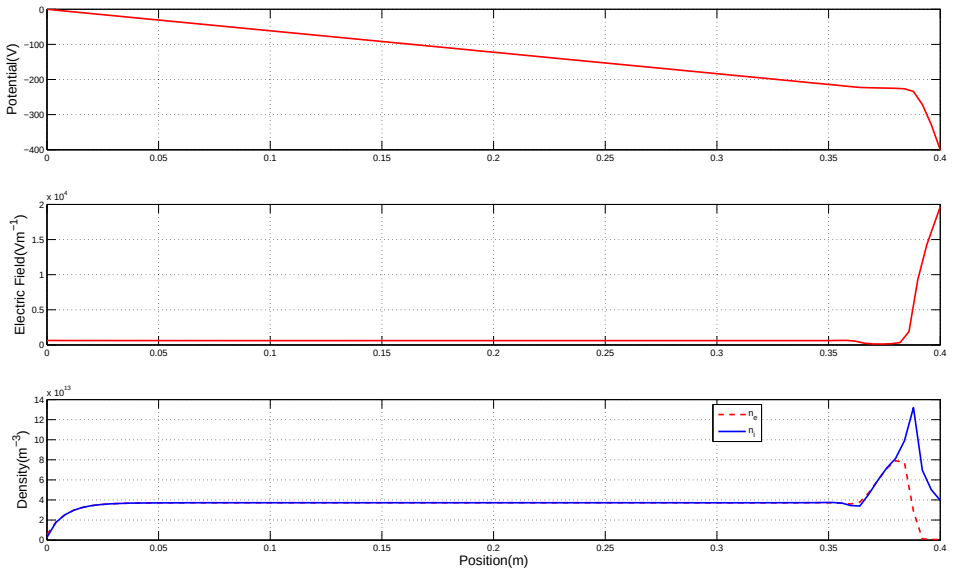

FIGURE 5.7: The results after 6×10^4 time steps

From Figure 5.4-5.7 we can see that the results are reaching a steady state. But to realize it we need to control the time step dynamically and it need a very long time. Although we didn't get a steady state, the phenomena we expect have appeared. In Figure 5.7 we can see the three regions from the right to the left: cathode fall (0.39-0.4 m), negative glow (0.37-0.39 m) and positive column (the rest). The potential is -400 V at the cathode and rises rapidly from the cathode. In the cathode fall region the electric filed is in the order of 10kV m^{-1}. The field is nearly zero in the negative glow. In the cathode fall the ions are accelerated by the electric field and hitting the cathode surface causing secondary emission. The electrons emitted from the cathode surface are accelerated by the electric field and are trapped in the negative glow and lose their energy in ionizing the plasma. So in the cathode fall region the density of electrons is very low. We also see the region of quasi-neutrality in the bulk where the densities of two particles are very close. Our results are similar with those given in [15].

5.3 Conclusion

We have presented a model to simulate the process of dc-discharge. We have got the results which we expect, but it's a pity that we didn't get a steady state. We will continue working on it till we get a steady state. Nevertheless, the results are meaningful. At the same time, it means that the homogeneous flux scheme even complete flux is a good method for the simulation of dc discharge.

Chapter 6

The finite volume scheme for advection-diffusion-reaction systems

In [9, 16] an integral representation has been derived for the flux of a scalar advection-diffusion-reaction equation from a local BVP for the *entire* equation, including the source term. As a consequence, the flux consists of two parts, i.e., a homogeneous and an inhomogeneous part, corresponding to the homogeneous and particular solution of the BVP, respectively. In this chapter, we extend the idea to systems. A representation of the numerical homogeneous flux and the finite volume scheme for one-dimensional advection-diffusion-reaction systems will be presented.

6.1 Finite Volume Discretisation

Consider the system of equations

$$(\boldsymbol{U}\boldsymbol{\varphi} - \mathcal{E}\boldsymbol{\varphi}')' = \boldsymbol{s}, \tag{6.1}$$

on the interval (a, b), where $\boldsymbol{U} := \begin{bmatrix} u_{11} & u_{12} \\ u_{21} & u_{22} \end{bmatrix}$ is the mass flux matrix, $\boldsymbol{\varphi} := \begin{bmatrix} \varphi_1 \\ \varphi_2 \end{bmatrix}$, $\mathcal{E} := \begin{bmatrix} \varepsilon_{11} & \varepsilon_{12} \\ \varepsilon_{21} & \varepsilon_{22} \end{bmatrix}$ the diffusion/conduction matrix and $\boldsymbol{s} := \begin{bmatrix} s_1 \\ s_2 \end{bmatrix}$ the (chemical) source term. We assume that $\boldsymbol{U}$ is invertible and $\mathcal{E}$ symmetric and positive definite and both are constant. We define $\boldsymbol{D} := \mathcal{E}^{-1}\boldsymbol{U}$ and assume that $\boldsymbol{D}$ is diagonalizable.

Associated with Eq. (6.1) we introduce the flux(vector) $\boldsymbol{f} := \begin{bmatrix} f_1 \\ f_2 \end{bmatrix}$, defined by

$$\boldsymbol{f} := \boldsymbol{U}\boldsymbol{\varphi} - \mathcal{E}\boldsymbol{\varphi}', \tag{6.2}$$

i.e.,

$$\begin{cases} f_1 = u_{11}\varphi_1 + u_{12}\varphi_2 - \varepsilon_{11}\varphi_1' - \varepsilon_{12}\varphi_2', \\ \\ f_2 = u_{21}\varphi_1 + u_{22}\varphi_2 - \varepsilon_{21}\varphi_1' - \varepsilon_{22}\varphi_2'. \end{cases} \tag{6.3}$$

Equation (6.1) reduces to $\boldsymbol{f}' = \boldsymbol{s}$. Integrating this over an arbitrary interval $[\alpha, \beta] \subset [a, b]$ we obtain the integral form of the conservation law, i.e.,

$$\boldsymbol{f}(\beta) - \boldsymbol{f}(\alpha) = \int_\alpha^\beta \boldsymbol{s}(x)dx. \tag{6.4}$$

In the finite volume method (FVM) we cover $[a, b]$ with a finite number of disjunct intervals I_j of size Δx and use the cell-centered approach to define the spatial grid x_j where the variable $\boldsymbol{\varphi}$ has to be approximated. We choose the grid point x_j in the center of the jth interval I_j. Consequently we have $I_j = [x_{j-1/2}, x_{j+1/2}]$ with $x_{j+1/2} = \frac{1}{2}(x_j + x_{j+1})$. Imposing the integral form Eq. (6.4) on each of the intervals I_j and adopting the following notation: variables defined in the grid points x_j and x_{j+1} are indicated with the subscripts C(center) and E(east), respectively, and variables at the cell edges $x_{j+1/2}$ and $x_{j-1/2}$ by the subscripts w (west) and e (east), respectively, we obtain the discrete conservation law

$$\boldsymbol{F}_e - \boldsymbol{F}_w = \boldsymbol{s}_C \Delta x, \tag{6.5}$$

where $\boldsymbol{s}_C := \boldsymbol{s}(x_j)$ and $\boldsymbol{F}_e$ is the numerical flux at $x = x_e$, etc. We used the midpoint rule for the integral in the right-hand side. In next section we complete the FVM with expressions for the numerical flux.

6.2 Representation for the Flux(vector)

First we summarize some properties of the exponential matrix $e^{\boldsymbol{A}}$ and exponential matrix function $e^{x\boldsymbol{A}}$ which will be used later in the derivation.

Property 6.1. *Let $\boldsymbol{A}$ and $\boldsymbol{B}$ be $n \times n$ matrices and $\boldsymbol{I}$ the identity matrix, then the following properties hold*

1. $[e^{\boldsymbol{A}}]^{-1}$ *exists, and* $[e^{\boldsymbol{A}}]^{-1} = e^{-\boldsymbol{A}}$.
2. *if* $\boldsymbol{AB} = \boldsymbol{BA}$, *then* $e^{\boldsymbol{A}}e^{\boldsymbol{B}} = e^{\boldsymbol{A}+\boldsymbol{B}}$;
3. *if* $\boldsymbol{B}$ *is invertible, then* $e^{\boldsymbol{BAB}^{-1}} = \boldsymbol{B}e^{\boldsymbol{A}}\boldsymbol{B}^{-1}$;
4. $\boldsymbol{A}e^{x\boldsymbol{A}} = e^{x\boldsymbol{A}}\boldsymbol{A}$;
5. $\frac{d}{dx}[e^{x\boldsymbol{A}}] = \boldsymbol{A}e^{x\boldsymbol{A}}$.

The derivation of the expression for the flux $\boldsymbol{F}_e$ at the eastern cell edge x_e located between the grid points x_C and x_E is based on the following model boundary value problem (BVP) for the unknown $\boldsymbol{\varphi}$:

$$(\boldsymbol{U}\boldsymbol{\varphi} - \mathcal{E}\boldsymbol{\varphi}')' = \boldsymbol{s}, \quad x_C < x < x_E, \tag{6.6a}$$

$$\boldsymbol{\varphi}(x_C) = \boldsymbol{\varphi}_C, \quad \boldsymbol{\varphi}(x_E) = \boldsymbol{\varphi}_E. \tag{6.6b}$$

From Eq. (6.2) and the definition of $\boldsymbol{D}$ we obtain $\boldsymbol{f} = -\mathcal{E}[\boldsymbol{\varphi}' - \boldsymbol{D}\boldsymbol{\varphi}]$. Integrating equation (6.6a) we get the following integral balance

$$\boldsymbol{f}(x) - \boldsymbol{f}(x_e) = \boldsymbol{S}(x) := \int_{x_e}^{x} \boldsymbol{s}(\xi)\mathrm{d}\xi. \tag{6.7}$$

From Property 6.1.4 and 6.1.5 we have $[e^{-x\boldsymbol{D}}\boldsymbol{\varphi}]' = e^{-x\boldsymbol{D}}[\boldsymbol{\varphi}' - \boldsymbol{D}\boldsymbol{\varphi}]$, so we have $\boldsymbol{f} = -\mathcal{E}e^{x\boldsymbol{D}}\left(e^{-x\boldsymbol{D}}\boldsymbol{\varphi}\right)'$. Substituting this into Eq. (6.7) we obtain

$$-\mathcal{E}e^{x\boldsymbol{D}}(e^{-x\boldsymbol{D}}\boldsymbol{\varphi})' - \boldsymbol{f}(x_e) = \boldsymbol{S}(x),$$

Using Property 6.1.1 we obtain

$$(e^{-x\boldsymbol{D}}\boldsymbol{\varphi})' + e^{-x\boldsymbol{D}}\mathcal{E}^{-1}\boldsymbol{f}(x_e) = -e^{-x\boldsymbol{D}}\mathcal{E}^{-1}\boldsymbol{S}(x).$$

Integrating the equation above from x_C to x_E we obtain

$$e^{-x_E\boldsymbol{D}}\boldsymbol{\varphi}_E - e^{-x_C\boldsymbol{D}}\boldsymbol{\varphi}_C + \left(\int_{x_C}^{x_E} e^{-x\boldsymbol{D}}\mathrm{d}x\right)\mathcal{E}^{-1}\boldsymbol{f}(x_e) = -\int_{x_C}^{x_E} e^{-x\boldsymbol{D}}\mathcal{E}^{-1}\boldsymbol{S}(x)\mathrm{d}x.$$

Left multiplication with $\boldsymbol{D}$ and applying Property 6.1.5, we obtain

$$\boldsymbol{D}(e^{-x_E\boldsymbol{D}}\boldsymbol{\varphi}_E - e^{-x_C\boldsymbol{D}}\boldsymbol{\varphi}_C) + \left(\int_{x_C}^{x_E} \boldsymbol{D}e^{-x\boldsymbol{D}}\mathrm{d}x\right)\mathcal{E}^{-1}\boldsymbol{f}(x_e) = -\boldsymbol{D}\int_{x_C}^{x_E} e^{-x\boldsymbol{D}}\mathcal{E}^{-1}\boldsymbol{S}(x)\mathrm{d}x,$$

i.e.,

$$(e^{-x_C\boldsymbol{D}} - e^{-x_E\boldsymbol{D}})\mathcal{E}^{-1}\boldsymbol{f}(x_e) = \boldsymbol{D}(e^{-x_C\boldsymbol{D}}\boldsymbol{\varphi}_C - e^{-x_E\boldsymbol{D}}\boldsymbol{\varphi}_E) - \boldsymbol{D}\int_{x_C}^{x_E} e^{-x\boldsymbol{D}}\mathcal{E}^{-1}\boldsymbol{S}(x)\mathrm{d}x.$$

Defining $\boldsymbol{P} := \Delta x \boldsymbol{D} = \Delta x \mathcal{E}^{-1} \boldsymbol{U}$, from Property 6.1.1, 6.1.2 and 6.1.5 we can obtain the following expression for the homogeneous flux $\boldsymbol{f}_e^h$

$$(e^{\boldsymbol{P}} - I)\mathcal{E}^{-1}\boldsymbol{f}_e^h = \boldsymbol{D}(e^{\boldsymbol{P}}\boldsymbol{\varphi}_C - \boldsymbol{\varphi}_E). \tag{6.8}$$

Simplifying this relation we get

$$\boldsymbol{f}_e^h = \boldsymbol{U}\left((I - e^{-\boldsymbol{P}})^{-1}\boldsymbol{\varphi}_C - (e^{\boldsymbol{P}} - I)^{-1}\boldsymbol{\varphi}_E\right). \tag{6.9}$$

In the following, we define some variables to express $\boldsymbol{f}_e^h$ in a form easily calculated. We denote the eigenvalues and eigenvectors of $\boldsymbol{D}$ by λ_1, λ_2 and $\boldsymbol{v}_1$, $\boldsymbol{v}_2$, respectively. Next we define $\Lambda := \begin{bmatrix} \lambda_1 & \\ & \lambda_2 \end{bmatrix}$, $\boldsymbol{V} := [\boldsymbol{v}_1, \boldsymbol{v}_2]$ and $\boldsymbol{M} := \Delta x \Lambda := \begin{bmatrix} \mu_1 & \\ & \mu_2 \end{bmatrix}$. So we have

$$\boldsymbol{D}\boldsymbol{V} = \boldsymbol{V}\Lambda,$$

and

$$\boldsymbol{P} = \Delta x \boldsymbol{D} = \boldsymbol{V}(\Delta x \Lambda)\boldsymbol{V}^{-1} = \boldsymbol{V}\boldsymbol{M}\boldsymbol{V}^{-1}. \tag{6.10}$$

We calculate the coefficient of $\boldsymbol{\varphi}_E$ first. From (6.10) and Property 6.1.3 we obtain

$$e^{\boldsymbol{P}} - I = \boldsymbol{V}e^{\boldsymbol{M}}\boldsymbol{V}^{-1} - \boldsymbol{V}\boldsymbol{V}^{-1} = \boldsymbol{V}(e^{\boldsymbol{M}} - I)\boldsymbol{V}^{-1},$$

and then the inverse of $e^{\boldsymbol{P}} - I$

$$\begin{aligned}
\left(e^{\boldsymbol{P}} - I\right)^{-1} &= \boldsymbol{V}[e^{\boldsymbol{M}} - I]^{-1}\boldsymbol{V}^{-1} \\
&= \boldsymbol{V}\begin{bmatrix} e^{\mu_1} - 1 & \\ & e^{\mu_2} - 1 \end{bmatrix}^{-1}\boldsymbol{V}^{-1} \\
&= \boldsymbol{V}\begin{bmatrix} 1/\mu_1 & \\ & 1/\mu_2 \end{bmatrix}\begin{bmatrix} \mu_1/(e^{\mu_1} - 1) & \\ & \mu_2/(e^{\mu_2} - 1) \end{bmatrix}\boldsymbol{V}^{-1} \\
&= \frac{1}{\Delta x}\boldsymbol{V}\Lambda^{-1}\begin{bmatrix} B(\mu_1) & \\ & B(\mu_2) \end{bmatrix}\boldsymbol{V}^{-1} \\
&= \frac{1}{\Delta x}\boldsymbol{D}^{-1}\boldsymbol{V}\begin{bmatrix} B(\mu_1) & \\ & B(\mu_2) \end{bmatrix}\boldsymbol{V}^{-1}.
\end{aligned}$$

Next we calculate the coefficient of $\boldsymbol{\varphi}_C$. From Eq. (6.10) we have

$$-\boldsymbol{P} = \boldsymbol{V}(-\Delta x \Lambda)\boldsymbol{V}^{-1} = \boldsymbol{V}(-\boldsymbol{M})\boldsymbol{V}^{-1},$$

so from Property 6.1.3

$$I - e^{-\boldsymbol{P}} = \boldsymbol{V}\boldsymbol{V}^{-1} - \boldsymbol{V}e^{-\boldsymbol{M}}\boldsymbol{V}^{-1} = \boldsymbol{V}(I - e^{-\boldsymbol{M}})\boldsymbol{V}^{-1},$$

and then the inverse of $I - e^{-\boldsymbol{P}}$

$$\begin{aligned}
\left(I - e^{-\boldsymbol{P}}\right)^{-1} &= \boldsymbol{V}(I - e^{-\boldsymbol{M}})^{-1}\boldsymbol{V}^{-1} \\
&= \boldsymbol{V}\begin{bmatrix} 1 - e^{-\mu_1} & \\ & 1 - e^{-\mu_2} \end{bmatrix}^{-1}\boldsymbol{V}^{-1} \\
&= \boldsymbol{V}\begin{bmatrix} -\mu_1^{-1} & \\ & -\mu_2^{-1} \end{bmatrix}\begin{bmatrix} -\mu_1/(1 - e^{-\mu_1}) & \\ & -\mu_2/(1 - e^{-\mu_2}) \end{bmatrix}\boldsymbol{V}^{-1} \\
&= \frac{1}{\Delta x}\boldsymbol{D}^{-1}\boldsymbol{V}\begin{bmatrix} B(-\mu_1) & \\ & B(-\mu_2) \end{bmatrix}\boldsymbol{V}^{-1},
\end{aligned}$$

where B is the Bernoulli function defined in Eq. (3.5). Note that B satisfies

$$B(-z) - B(z) = z. \tag{6.11}$$

We define

$$B(\boldsymbol{P}) := \boldsymbol{V}B(\boldsymbol{M})\boldsymbol{V}^{-1},$$

where

$$B(\boldsymbol{M}) = \begin{bmatrix} B(\mu_1) & \\ & B(\mu_2) \end{bmatrix}.$$

Then we obtain

$$-\boldsymbol{U}\left(e^{\boldsymbol{P}} - I\right)^{-1} = -\frac{1}{\Delta x}\boldsymbol{U}\boldsymbol{D}^{-1}B(\boldsymbol{P}) \quad \text{and} \quad \boldsymbol{U}\left(I - e^{-\boldsymbol{P}}\right)^{-1} = \frac{1}{\Delta x}\boldsymbol{U}\boldsymbol{D}^{-1}B(-\boldsymbol{P}).$$

Thus we obtain the following expression for the homogenous flux

$$\boldsymbol{f}_e^h = \frac{1}{\Delta x}\mathcal{E}[B(-\boldsymbol{P})\boldsymbol{\varphi}_C - B(\boldsymbol{P})\boldsymbol{\varphi}_E]. \tag{6.12}$$

Substituting Eq. (6.12) and a similar expression for $\boldsymbol{f}_w^h$ into Eq. (6.5) we obtain the homogeneous flux (HF) scheme

$$-A_W\boldsymbol{\varphi}_W + A_C\boldsymbol{\varphi}_C - A_E\boldsymbol{\varphi}_E = \Delta x^2\boldsymbol{s}_C, \tag{6.13}$$

where $A_W := \mathcal{E}B(-\boldsymbol{P})$, $A_E := \mathcal{E}B(\boldsymbol{P})$ and $A_C := A_W + A_E$. Applying it to every spatial grid point x_j results in the following linear system

$$\boldsymbol{A}\boldsymbol{\varphi} = \boldsymbol{b},$$

where $\boldsymbol{\varphi}$ and $\boldsymbol{b}$ are the vector of unknowns and source terms, respectively, and where the vector $\boldsymbol{b}$ contains in addition the boundary data. Note that the matrix $\boldsymbol{A}$ is a block matrix and every block is a 2×2 matrix.

Next we analyse the truncation error σ. Substituting the exact solution restricted to the grid, denoted by $\boldsymbol{\varphi}_h$, into FV scheme (6.13) and let $h = \Delta x$ we get the defect

$$
\begin{aligned}
h^2\boldsymbol{\sigma} =& - \mathcal{E}B(-\boldsymbol{P})\boldsymbol{\varphi}_h(x-h) + \mathcal{E}\Big(B(-\boldsymbol{P}) + B(\boldsymbol{P})\Big)\boldsymbol{\varphi}_h(x) - \mathcal{E}B(\boldsymbol{P})\boldsymbol{\varphi}_h(x+h) - h^2\boldsymbol{s}(x) \\
=& - \mathcal{E}B(-\boldsymbol{P})\Big(\boldsymbol{\varphi}_h(x) - h\boldsymbol{\varphi}_h'(x) + \frac{h^2}{2!}\boldsymbol{\varphi}_h''(x) - \frac{h^3}{3!}\boldsymbol{\varphi}_h^{(3)}(x) + \frac{h^4}{4!}\boldsymbol{\varphi}_h^{(4)}(x) + \cdots\Big) \\
& + \mathcal{E}\Big(B(-\boldsymbol{P}) + B(\boldsymbol{P})\Big)\boldsymbol{\varphi}_h(x) \\
& - \mathcal{E}B(\boldsymbol{P})\Big(\boldsymbol{\varphi}_h(x) + h\boldsymbol{\varphi}_h'(x) + \frac{h^2}{2!}\boldsymbol{\varphi}_h''(x) + \frac{h^3}{3!}\boldsymbol{\varphi}_h^{(3)}(x) + \frac{h^4}{4!}\boldsymbol{\varphi}_h^{(4)}(x) + \cdots\Big) - h^2\boldsymbol{s}(x) \\
=& \mathcal{E}\Big(B(-\boldsymbol{P}) - B(\boldsymbol{P})\Big)h\boldsymbol{\varphi}_h'(x) - \mathcal{E}\Big(B(-\boldsymbol{P}) + B(\boldsymbol{P})\Big)\frac{h^2}{2}\boldsymbol{\varphi}_h''(x) + \mathcal{E}\Big(B(-\boldsymbol{P}) - B(\boldsymbol{P})\Big)\frac{h^3}{6}\boldsymbol{\varphi}_h^{(3)}(x) \\
& - \mathcal{E}\Big(B(-\boldsymbol{P}) + B(\boldsymbol{P})\Big)\frac{h^4}{24}\boldsymbol{\varphi}_h^{(4)}(x) - h^2\boldsymbol{s}(x) + \cdots,
\end{aligned}
$$

We simplify the coefficients of the derivatives of $\boldsymbol{\varphi}_h'(x)$.

$$
\begin{aligned}
B(-\boldsymbol{P}) - B(\boldsymbol{P}) =& \boldsymbol{V}\begin{bmatrix} B(-\mu_1) & \\ & B(-\mu_2) \end{bmatrix}\boldsymbol{V}^{-1} - \boldsymbol{V}\begin{bmatrix} B(\mu_1) & \\ & B(\mu_2) \end{bmatrix}\boldsymbol{V}^{-1} \\
=& \boldsymbol{V}\begin{bmatrix} B(-\mu_1) - B(\mu_1) & \\ & B(-\mu_2) - B(\mu_2) \end{bmatrix}\boldsymbol{V}^{-1} \\
=& \boldsymbol{V}\begin{bmatrix} \mu_1 & \\ & \mu_2 \end{bmatrix}\boldsymbol{V}^{-1} \\
=& h\boldsymbol{V}\begin{bmatrix} \lambda_1 & \\ & \lambda_2 \end{bmatrix}\boldsymbol{V}^{-1} \\
=& h\boldsymbol{D}
\end{aligned}
$$

and using Taylor expansion

$$
\begin{aligned}
B(-\boldsymbol{P}) + B(\boldsymbol{P}) =& \boldsymbol{V}\begin{bmatrix} B(-\mu_1) + B(\mu_1) & \\ & B(-\mu_2) + B(\mu_2) \end{bmatrix}\boldsymbol{V}^{-1} \\
=& \boldsymbol{V}\begin{bmatrix} 2 + \frac{1}{6}\mu_1^2 + \frac{1}{360}\mu_1^4 + \cdots & \\ & 2 + \frac{1}{6}\mu_2^2 + \frac{1}{360}\mu_2^4 + \cdots \end{bmatrix}\boldsymbol{V}^{-1} \\
=& 2\boldsymbol{I} + \frac{1}{6}\boldsymbol{V}\begin{bmatrix} \mu_1^2 & \\ & \mu_2^2 \end{bmatrix}\boldsymbol{V}^{-1} + \frac{1}{360}\boldsymbol{V}\begin{bmatrix} \mu_1^4 & \\ & \mu_2^4 \end{bmatrix}\boldsymbol{V}^{-1} + \cdots \\
=& 2\boldsymbol{I} + \frac{1}{6}h^2\boldsymbol{D}^2 + \frac{1}{360}h^4\boldsymbol{D}^4 + \cdots.
\end{aligned}
$$

Substituting the result above in the expression of $h^2\boldsymbol{\sigma}$ we obtain

$$\begin{aligned}h^2\boldsymbol{\sigma} =&h^2\mathcal{E}\boldsymbol{D}\boldsymbol{\varphi}_h'(x) - \mathcal{E}\Big(2\boldsymbol{I} + \frac{1}{6}h^2\boldsymbol{D}^2 + \frac{1}{360}h^4\boldsymbol{D}^4 + \cdots\Big)\frac{h^2}{2}\boldsymbol{\varphi}_h''(x) + \mathcal{E}\boldsymbol{D}\frac{h^4}{6}\boldsymbol{\varphi}_h^{(3)}(x)\\ &- \mathcal{E}\Big(2\boldsymbol{I} + \frac{1}{6}h^2\boldsymbol{D}^2 + \frac{1}{360}h^4\boldsymbol{D}^4 + \cdots\Big)\frac{h^4}{24}\boldsymbol{\varphi}_h^{(4)}(x) - h^2\boldsymbol{s}(x) + \cdots\\ =&h^2\left(\Big(\boldsymbol{U}\boldsymbol{\varphi}_h'(x) - \mathcal{E}\boldsymbol{\varphi}_h''(x) - \boldsymbol{s}(x)\Big) - h^2\Big(\frac{\mathcal{E}\boldsymbol{D}^2}{12}\boldsymbol{\varphi}_h''(x) + \frac{\mathcal{E}}{12}\boldsymbol{\varphi}_h^{(4)}(x) - \frac{\boldsymbol{U}}{6}\boldsymbol{\varphi}_h^{(3)}(x)\Big) + \mathcal{O}(h^4)\right).\end{aligned}$$

So the truncation error is

$$\boldsymbol{\sigma} = -h^2\left(\frac{\mathcal{E}\boldsymbol{D}^2}{12}\boldsymbol{\varphi}_h''(x) + \frac{\mathcal{E}}{12}\boldsymbol{\varphi}_h^{(4)}(x) - \frac{\boldsymbol{U}}{6}\boldsymbol{\varphi}_h^{(3)}(x)\right) + \mathcal{O}(h^4). \tag{6.14}$$

We obtain that the local error of the homogeneous flux scheme (6.14) is second-order. We should note that in Eq. (6.14) the coefficient of h^2 is dependent on $\mathcal{E}$. The first term in (6.14)

$$-h^2\frac{\mathcal{E}\boldsymbol{D}^2}{12}\boldsymbol{\varphi}_h''(x) = -h^2\frac{\boldsymbol{U}\mathcal{E}^{-1}\boldsymbol{U}}{12}\boldsymbol{\varphi}_h''(x) = -h\frac{\boldsymbol{U}\boldsymbol{P}}{12}\boldsymbol{\varphi}_h''(x) \tag{6.15}$$

This would reduce the accurate order for the dominant advection problems.

6.3 Extension to Singular Mass Flux Matrix

Consider the system of equations

$$(\boldsymbol{U}\boldsymbol{\varphi} - \mathcal{E}\boldsymbol{\varphi}')' = \boldsymbol{s}, \tag{6.16}$$

on the interval (a, b), where $\boldsymbol{U} := \begin{bmatrix} 0 & 0 & 0\\ 0 & u_{22} & 0\\ 0 & 0 & u_{33}\end{bmatrix}$, $\boldsymbol{\varphi} := \begin{bmatrix}\varphi_1\\ \varphi_2\\ \varphi_3\end{bmatrix}$, $\mathcal{E} := \begin{bmatrix}\varepsilon_{11} & \varepsilon_{12} & \varepsilon_{13}\\ \varepsilon_{21} & \varepsilon_{22} & \varepsilon_{23}\\ \varepsilon_{31} & \varepsilon_{32} & \varepsilon_{33}\end{bmatrix}$, $\boldsymbol{s} := \begin{bmatrix}s_1\\ s_2\\ s_3\end{bmatrix}$ and u_{22}, $u_{33} \neq 0$. We assume that $\boldsymbol{U}$, $\mathcal{E}$ and $\boldsymbol{s}$ are constant and $\mathcal{E}$ is symmetric and positive definite. We should note that $\boldsymbol{U}$ is singular, so we can't apply the result of the previous section to this case directly. We will discretize the second and the third equation by the scheme (6.14) together with central scheme and the first equation by the central scheme.

First we introduce some notions. $\boldsymbol{f} := \begin{bmatrix}f_1\\ f_2\\ f_3\end{bmatrix}$ the flux, defined by

$$\boldsymbol{f} = \boldsymbol{U}\boldsymbol{\varphi} - \mathcal{E}\boldsymbol{\varphi}', \tag{6.17}$$

i.e.,

$$\begin{cases} f_1 = & -\varepsilon_{11}\varphi_1' - \varepsilon_{12}\varphi_2' - \varepsilon_{13}\varphi_3', \\ f_2 = u_{22}\varphi_2 & -\varepsilon_{21}\varphi_1' - \varepsilon_{22}\varphi_2' - \varepsilon_{23}\varphi_3', \\ f_2 = u_{33}\varphi_3 & -\varepsilon_{31}\varphi_1' - \varepsilon_{32}\varphi_2' - \varepsilon_{33}\varphi_3'. \end{cases} \tag{6.18}$$

$\boldsymbol{g} := \begin{bmatrix} g_1 \\ g_2 \end{bmatrix}$ the new flux for φ_2 and φ_3 excluding φ_1-term , defined by

$$\begin{cases} g_1 = u_{22}\varphi_2 - \varepsilon_{22}\varphi_2' - \varepsilon_{23}\varphi_3', \\ g_2 = u_{33}\varphi_3 - \varepsilon_{32}\varphi_2' - \varepsilon_{33}\varphi_3'. \end{cases} \tag{6.19}$$

$\boldsymbol{t} := \begin{bmatrix} t_1 \\ t_2 \end{bmatrix}$ the new reaction term for φ_2 and φ_3, defined by

$$\begin{cases} t_1 = s_2 + \varepsilon_{21}\varphi_1'', \\ t_2 = s_3 + \varepsilon_{31}\varphi_1''. \end{cases} \tag{6.20}$$

We apply the scheme (6.14) to the system

$$(\boldsymbol{U}^*\boldsymbol{\varphi}^* - \mathcal{E}^*\boldsymbol{\varphi}^{*'})' = \boldsymbol{t}, \tag{6.21}$$

where $\boldsymbol{U}^* := \begin{bmatrix} u_{22} & 0 \\ 0 & u_{33} \end{bmatrix}$, $\mathcal{E}^* := \begin{bmatrix} \varepsilon_{22} & \varepsilon_{23} \\ \varepsilon_{32} & \varepsilon_{33} \end{bmatrix}$ and $\boldsymbol{\varphi}^* := \begin{bmatrix} \varphi_2 \\ \varphi_3 \end{bmatrix}$. After discretization we obtain

$$-A_W^*\boldsymbol{\varphi}_W^* + A_C^*\boldsymbol{\varphi}_C^* - A_E^*\boldsymbol{\varphi}_E^* = \Delta x^2 \boldsymbol{t}_C, \tag{6.22}$$

where $A_W^* := \mathcal{E}^* B(-\boldsymbol{P}^*)$, $A_E^* := \mathcal{E}^* B(\boldsymbol{P}^*)$, $A_C^* := A_W^* + A_E^*$ and $\boldsymbol{P}^* := \Delta x \mathcal{E}^{*-1}\boldsymbol{U}^*$.

Next we apply the central scheme to the second order derivative of φ_1 in $\boldsymbol{t}$ and to the first equation of the system to obtain

$$\begin{aligned} &-\begin{bmatrix} \varepsilon_{21} \\ \varepsilon_{31} \end{bmatrix}\varphi_{1,W} - A_W^*\boldsymbol{\varphi}_W^* + 2\begin{bmatrix} \varepsilon_{21} \\ \varepsilon_{31} \end{bmatrix}\varphi_{1,C} + A_C^*\boldsymbol{\varphi}_C^* \\ &-\begin{bmatrix} \varepsilon_{21} \\ \varepsilon_{31} \end{bmatrix}\varphi_{1,E} - A_E^*\boldsymbol{\varphi}_E^* = \Delta x^2 \begin{bmatrix} s_{2,C} \\ s_{3,C} \end{bmatrix}, \end{aligned} \tag{6.23}$$

and

$$\begin{aligned} &-\varepsilon_{11}\varphi_{1,W}-\varepsilon_{12}\varphi_{2,W}-\varepsilon_{13}\varphi_{3,W}+2\varepsilon_{11}\varphi_{1,C}+2\varepsilon_{12}\varphi_{2,C}+2\varepsilon_{13}\varphi_{3,C} \\ &-\varepsilon_{11}\varphi_{1,E}-\varepsilon_{12}\varphi_{2,E}-\varepsilon_{13}\varphi_{3,E}=\Delta x^2 s_{1,C}. \end{aligned} \tag{6.24}$$

Writing Eq. (6.22) and Eq. (6.23) together we can obtain the discretization of system (6.16)

$$-A_W\boldsymbol{\varphi}_W+A_C\boldsymbol{\varphi}_C-A_E\boldsymbol{\varphi}_E=\Delta x^2\boldsymbol{s}_C, \tag{6.25}$$

where $A_W := \begin{bmatrix} \varepsilon_{11} & \varepsilon_{12} & \varepsilon_{13} \\ \varepsilon_{21} & A^*_{W11} & A^*_{W12} \\ \varepsilon_{31} & A^*_{W21} & A^*_{W22} \end{bmatrix}$, $A_E := \begin{bmatrix} \varepsilon_{11} & \varepsilon_{12} & \varepsilon_{13} \\ \varepsilon_{21} & A^*_{E11} & A^*_{E12} \\ \varepsilon_{31} & A^*_{E21} & A^*_{E22} \end{bmatrix}$, $A_C := A_W + A_E$ and A^*_{W11}, A^*_{E11} etc. are the entries of matrix A_W and A_E. Because the central scheme is also second-order, the scheme (6.25) should be second-order. This will be tested in the numerical experiment.

6.4 Numerical Examples

In this section we apply the HF scheme to the model problem Eq. (6.1) to compare the numerical result with the exact solution.

First we choose $\boldsymbol{U} = \begin{bmatrix} 3 & 4 \\ 5 & 6 \end{bmatrix}$ and $\mathcal{E} = \frac{1}{2}\varepsilon \begin{bmatrix} 3 & -1 \\ -1 & 3 \end{bmatrix}$ and source term $\boldsymbol{s}$ and boundary conditions chosen such that the exact solution is given by $\varphi_1 = 1 - e^{(x-1)/\alpha}$ and $\varphi_2 = e^{(x-1)/\beta}$ where α and β are constants. From Figure 6.1-6.3 we can see that the HF scheme can approximate the exact solution well even if in the case of dominant advection.

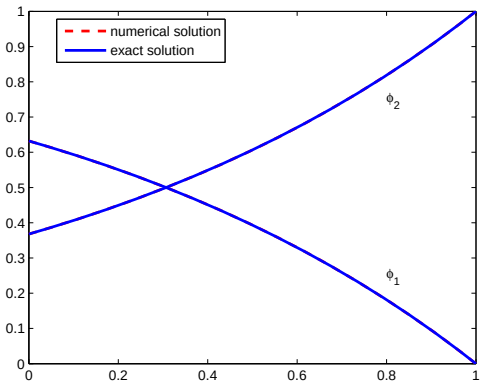

FIGURE 6.1: Numerical and exact solutions. Parameter values are $\varepsilon = 1$, $\alpha = 1$, $\beta = 1$ and $\Delta x = 0.01$

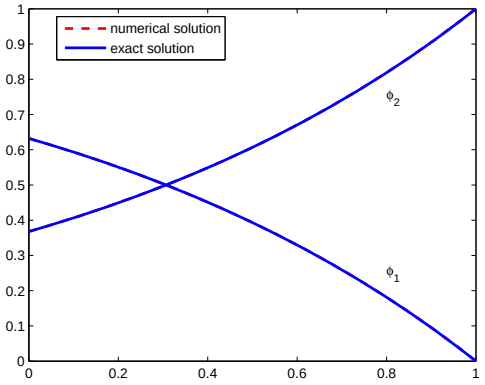

FIGURE 6.2: Numerical and exact solutions. Parameter values are $\varepsilon = 10^{-2}$, $\alpha = 1$, $\beta = 1$ and $\Delta x = 0.01$

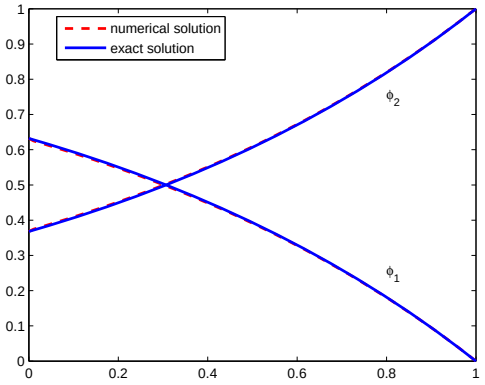

FIGURE 6.3: Numerical and exact solutions. Parameter values are $\varepsilon = 10^{-8}$, $\alpha = 1$, $\beta = 1$ and $\Delta x = 0.01$

Now we test the result obtained in Section 6.3. we choose $\boldsymbol{U} = \begin{bmatrix} 0 & 0 & 0 \\ 0 & 3 & 0 \\ 0 & 0 & 5 \end{bmatrix}$ and $\mathcal{E} = \varepsilon \begin{bmatrix} 4 & 2 & -1 \\ 2 & 4 & -1 \\ -1 & -1 & 4 \end{bmatrix}$ and source term $\boldsymbol{s}$ and boundary condition chosen such that the exact solution is given by $\varphi_1 = x^{15}$, $\varphi_2 = 1 - e^{(x-1)/\alpha}$ and $\varphi_3 = e^{(x-1)/\beta}$ where α and β are constants. The results are given in Figure 6.4-6.6 and Table 6.1-6.3.

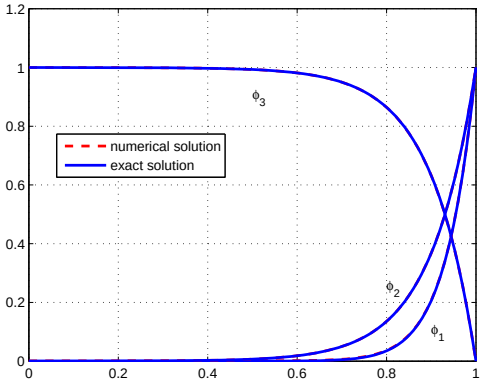

FIGURE 6.4: Numerical and exact solutions. Parameter values are $\varepsilon = 1$, $\alpha = 0.1$, $\beta = 0.1$ and $\Delta x = 0.01$

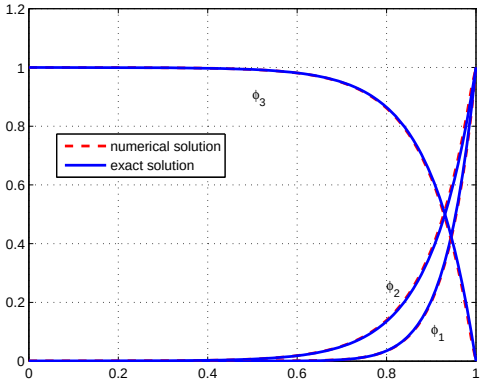

FIGURE 6.5: Numerical and exact solutions. Parameter values are $\varepsilon = 10^{-2}$, $\alpha = 0.1$, $\beta = 0.1$ and $\Delta x = 0.01$

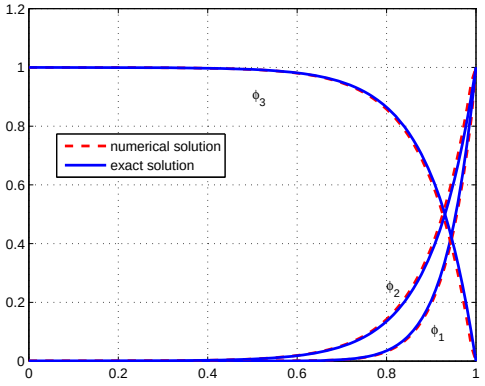

FIGURE 6.6: Numerical and exact solutions. Parameter values are $\varepsilon = 10^{-8}$, $\alpha = 0.1$, $\beta = 0.1$ and $\Delta x = 0.01$

Δx	$\|\phi_1 - u_1\|_\infty$	$\|\phi_2 - u_2\|_\infty$	$\|\phi_3 - u_3\|_\infty$
10^{-1}	14.631e-002	1.2917e-002	1.6792e-002
10^{-2}	15.706e-004	1.4044e-004	1.7954e-004
10^{-3}	15.719e-006	1.4050e-006	1.7964e-006

TABLE 6.1: The absolute error. Parameter values are $\varepsilon = 1$, $\alpha = 0.1$, $\beta = 0.1$

Δx	$\|\phi_1 - u_1\|_\infty$	$\|\phi_2 - u_2\|_\infty$	$\|\phi_3 - u_3\|_\infty$
10^{-1}	1.2847e-001	1.9633e-001	2.0144e-001
10^{-2}	1.5465e-002	2.2310e-002	2.4816e-002
10^{-3}	1.9196e-004	2.6404e-004	3.2066e-004

TABLE 6.2: The absolute error. Parameter values are $\varepsilon = 10^{-2}$, $\alpha = 0.1$, $\beta = 0.1$

Δx	$\|\phi_1 - u_1\|_\infty$	$\|\phi_2 - u_2\|_\infty$	$\|\phi_3 - u_3\|_\infty$
10^{-1}	1.2699e-001	2.1407e-001	2.1407e-001
10^{-2}	3.0418e-002	4.5993e-002	4.5993e-002
10^{-3}	3.3052e-003	4.9582e-003	3.3052e-003

TABLE 6.3: The absolute error. Parameter values are $\varepsilon = 10^{-8}$, $\alpha = 0.1$, $\beta = 0.1$

From the tables above we can see that the homogeneous flux scheme is second-order when $\varepsilon = 1$ and as ε decreases the convergence order reduces to one. This is because the coefficient of second-order term in the truncation error is dependent on ε as we mentioned in Section 6.2.

6.5 Summary and Conclusions

We have derived an expression for the homogeneous flux for the systems of advection-diffusion-reaction equations from a local BVP for the entire equation. In the future work we can also give the expression for inhomogeneous flux and obtain the finite volume-complete flux scheme, like in [9, 16]. We can also extend it to time-dependent problems.

Bibliography

[1] F.F. Chen. *Introduction to Plasma Physics and Controlled Fusion*, volume 1. Plenum Press, New York, second edition, 1984.

[2] D.A. Gurnett and Amitava Bhattacharjee. *Introduction to Plasma Physics With Space and Laboratory Applications*. Cambridge University Press, Cambridge, 2005.

[3] J.D.P. Passchier and W.J. Goedheer. A two-dimensional fluid model for an argon rf discharge. *J. Appl. Phys.*, 74(6):3744, 1993.

[4] M. Surendra, D.B. Graves, and G.M. Jellum. Self-consistent model of a direct-current glow discharge: Treatment of fast electrons. *Phys. Ref. A*, 41(2):1112, 1990.

[5] C. Punset, J.-P. Boeuf, and L.C. Pitchford. Two dimensional simulation of an alternating current matrix plasma display cell: Cross-talk and other geometric effects. *J. Appl. Phys.*, 83(4):1884–1897, 1998.

[6] J.P. Boeuf and L.C. Pitchford. Two-dimensional model of a capacitively coupled rf discharge and comparisons with experiments in the gaseous electronics conference reference reactor. *Phys. Ref. E*, 51(2):1376, 1995.

[7] Ph. Belenguer J. Meunier and J.P. Boeuf. Numerical model of an ac plasma display panel cell in neon-xenon mixtures. *J. Appl. Phys.*, 78:731, 1995.

[8] R. Veerasingam, R.B. Campbell, and R.T. McGrath. One-dimensional fluid simulations of a helium-xenon filled ac colour plasma flat panel display pixel. *Plasma Sources Sci. Technol.*, 6:157–169, 1997.

[9] J.H.M. ten Thije Boonkkamp and M.J.H. Anthonissen. The finite volume-complete flux scheme for one-dimensional advection-diffusion-reaction equations. *CASA report*, 08-28, 2008.

[10] L. Fox and D.F. Mayers. *Numerical Solution for Ordinary Differential Equations*. Chapman and Hall, 1987.

[11] U.M. Ascher, R.M.M. Mattheij, and R.D. Russel. *Numerical Solution of Boundary Value Problems for Ordinary Differential Equations.* Prentice Hall, 1988.

[12] M.E. Kramer. *Aspects of Sloving Non-Linear Boundary Value Porblems Numerically.* PhD thesis, Eindhoven University of Technology, 1992.

[13] M. Graziadei. *Using Local Defect Correction for laminar flame simulation.* PhD thesis, Eindhoven University of Technology, 2004.

[14] P.T. Boggs. The solution of non-linear systems of equations by a-stable integration techniques. *SIAM J. Numer. Analysis*, 8(767-785), 1971.

[15] Y.P. Raizer. *Gas Discharge Physics.* Springer-Verlag, 1991.

[16] B. van 't Hof, J.H.M. ten Thije Boonkkamp, and R.M.M. Mattheij. Discretisation of the stationary convection-diffusion-reaction equation. *Numer. Meth. for Part. Diff. Eq.*, 14:607–625, 1998.